

Supplementary Information

S1. Physicochemical and spectroscopic data of 1–5

Curvularin (1): White tabular crystals (from MeOH), m.p. 199–200 °C, $[\alpha]_D^{20} -34.1$ (*c* 0.7, EtOH) and $[\alpha]_D^{20} -38.3$ (*c* 1.2, MeOH). Positive ESI-MS *m/z*: 293 [M + H]⁺, 315 [M + Na]⁺; negative ESI-MS *m/z*: 291 [M + Cl]⁻. ¹H NMR (400 MHz, acetone-*d*₆) δ: 9.09 (1H, br s, HO-7), 8.76 (1H, br s, HO-5), 6.38 (1H, d, *J* = 2.3 Hz, H-6), 6.35 (1H, d, *J* = 2.3 Hz, H-4), 4.96–4.87 (1H, m, H-15), 3.78 (1H, d, *J* = 15.7 Hz, Ha-2), 3.70 (1H, d, *J* = 15.7 Hz, Hb-2), 3.11 (1H, ddd, *J* = 15.5, 8.4, 3.0 Hz, Ha-10), 2.77 (1H, ddd, *J* = 15.5, 9.7, 2.9 Hz, Hb-10), 1.80–1.20 (8H, m, H₂-11 → H₂-14), 1.11 (3H, d, *J* = 6.3 Hz, H₃-16). ¹³C NMR (400 MHz, acetone-*d*₆) δ: 206.7 (C-9), 171.0 (C-1), 160.1 (C-5), 158.2 (C-7), 136.9 (C-3), 121.3 (C-8), 112.2 (C-4), 102.5 (C-6), 72.5 (C-15), 43.9 (C-10), 39.7 (C-2), 32.8 (C-14), 27.5 (C-12), 24.5 (C-13), 23.4 (C-11), 20.6 (C-16).

Citrinin (2): Lemon yellow needles (MeOH), m.p. 179–180 °C, $[\alpha]_D^{20} -20.1$ (*c* 0.5, EtOH). Positive ESI-MS *m/z*: 251 [M + H]⁺, 273 [M + Na]⁺; negative ESI-MS *m/z*: 249 [M – H]⁻. ¹H NMR (400 MHz, CDCl₃) δ: 15.88 (1H, s, HO-12), 15.11 (1H, s, HO-8), 8.23 (1H, s, H-1), 4.77 (1H, q, *J* = 6.7 Hz, H-3), 2.98 (1H, q, *J* = 7.2 Hz, H-4), 2.02 (3H, s, H₃-11), 1.34 (3H, d, *J* = 6.7 Hz, H₃-9), 1.22 (3H, d, *J* = 7.2 Hz, H₃-10). ¹³C NMR (100 MHz, CDCl₃) δ: 184.0 (C-6), 177.3 (C-8), 174.7 (C-12), 162.9 (C-1), 139.2 (C-4a), 123.2 (C-5), 107.5 (C-8a), 100.5 (C-7), 81.8 (C-3), 34.7 (C-4), 9.6 (C-10), 18.4 (C-9), 18.7 (C-11).

Penicitrinone A (3): An orange crystalline powder (MeOH), m.p. 153–155 °C, $[\alpha]_D^{20} +81.3$ (*c* 0.2, MeOH). Positive ESI-MS *m/z*: 381 [M + H]⁺; negative ESI-MS *m/z*: 379 [M – H]⁻. ¹H NMR (400 MHz, CDCl₃) δ: 8.34 (1H, br s, HO-5'), 6.38 (1H, s, H-7), 4.97 (1H, br q, *J* = 6.6 Hz, H-3), 4.61 (1H, qd, *J* = 6.7, 4.1 Hz, H-2'), 3.16 (1H, qd, *J* = 6.7, 4.1 Hz, H-3'), 3.12 (1H, br q, *J* = 7.0 Hz, H-4), 2.20 (3H, s, H₃-10'), 2.11 (3H, s, H₃-11), 1.43 (3H, d, *J* = 6.4 Hz, H₃-9), 1.42 (3H, d, *J* = 6.2 Hz, H₃-8'), 1.33 (3H, d, *J* = 6.9 Hz, H₃-9'), 1.31 (3H, d, *J* = 7.0 Hz, H₃-10). ¹³C NMR (100 MHz, CDCl₃) δ: 184.5 (C-6), 158.2 (C-8), 155.7 (C-1), 147.6 (C-5'), 139.5 (C-3'a), 138.0 (C-7'a), 135.9 (C-7'), 132.0 (C-5), 131.0 (C-4a), 116.6 (C-4'), 103.4 (C-7), 102.4 (C-6'), 100.2 (C-8a), 88.1 (C-2'), 82.5 (C-3), 44.8 (C-3'), 35.1 (C-4), 21.1 (C-9), 19.2 (C-9'), 19.1 (C-10), 19.0 (C-8'), 11.6 (C-10'), 10.9 (C-11).

Erythro-23-O-methylneocyclocitrinol (4): yellowish solid (MeOH), $[\alpha]_D^{20} +87.9$ (*c* 1.2, MeOH). Positive ESIMS *m/z*: 415 [M + H]⁺, 437 [M + Na]⁺; negative ESI-MS *m/z*: 413 [M – H]⁻. ¹H NMR (400 MHz, DMSO-*d*₆) δ: 5.56 (1H, dd, *J* = 8.3, 6.3 Hz, H-1), 5.43 (1H, s, H-7), 5.12 (1H, d, *J* = 9.0 Hz, H-22), 4.63 (1H, d, *J* = 4.3 Hz, HO-3), 4.44 (1H, d, *J* = 4.9 Hz, HO-24), 3.79/3.77 (1H, dd, *J* = 8.9, 4.0 Hz, H-23), 3.65–3.56 (1H, m, H-24), 3.16/3.15 (3H, s, CH₃O-23), 3.15–3.07 (1H, m, H-3), 2.85 (1H, dd, *J* = 11.6, 5.5 Hz, H-9), 2.71–2.65 (1H, m, H-5), 2.63 (1H, br d, *J* = 13.0, Ha-4), 2.48 (2H, br s, H₂-18), 2.39–2.27 (2H, m, H_β-2 and H-17), 2.26 (1H, br t, *J* = 9.0 Hz, H-14), 2.11–2.01 (1H, m, Ha-2), 1.90–1.62 (4H, m, H_β-11, H_β-12 and H₂-16), 1.68 (3H, s, H₃-21), 1.62–1.42 (5H, m, H_β-4, Ha-11, Ha-12 and H₂-15), 0.99/0.97 (3H, d, *J* = 6.3 Hz, H₃-25), 0.54/0.53 (3H, s, H₃-19). ¹³C NMR (100 MHz, DMSO-*d*₆) δ: 204.2 (C-6), 156.96/156.98 (C-8), 145.6 (C-10), 138.71/138.82 (C-20), 124.4/124.3 (C-22), 124.3 (C-7), 122.1 (C-1), 81.3/81.4 (C-23), 68.32/68.38 (C-24), 63.1 (C-3), 58.87/58.92 (C-17), 55.5 (CH₃O-23), 54.4 (C-14), 53.3 (C-9), 48.1 (C-5), 46.78/46.80 (C-13), 41.4 (C-4), 37.08/37.13 (C-12), 36.0 (C-2), 27.5 (C-11), 27.2 (C-18), 23.8 (C-16), 22.36/22.40 (C-15), 19.0/18.8 (C-25), 18.29/18.07 (C-21), 13.47/13.51 (C-19).

*22E-7 α -Methoxy-5 α ,6 α -epoxyergosta-8(14),22-dien-3 β -ol (**5**):* $[\alpha]_D^{25} -53.6$ (*c* 0.4, CHCl₃). Positive ESI-MS *m/z*: 465 [M + Na]⁺. ¹H NMR (400 MHz, CDCl₃) δ : 5.22 (1H, dd, *J* = 15.2, 6.8 Hz, H-22), 5.17 (1H, dd, *J* = 15.2, 7.5 Hz, H-23), 4.16 (1H, d, *J* = 3.0 Hz, H-7), 3.93 (1H, tt, *J* = 11.6, 4.6 Hz, H-3), 3.41 (3H, s, CH₃O-7), 3.20 (1H, d, *J* = 3.0 Hz, H-6), 2.57–2.45 (1H, m, Ha-15), 2.43–2.36 (1H, m, H-9), 2.25–2.15 (1H, m, Hb-15), 2.14 (1H, dd, *J* = 13.0, 11.6 Hz, Ha-4), 2.13–2.07 (1H, m, H-20), 2.00–1.80 (3H, m, Ha-2, Ha-12, H-24), 1.75–1.60 (2H, m, Ha-1, Ha-16), 1.59–1.20 (9H, m, Hb-1, Hb-2, Hb-4, H₂-11, Ha-12, Hb-16, H-17, H-25), 1.01 (3H, d, *J* = 6.7 Hz, H₃-21), 0.91 (3H, d, *J* = 6.8 Hz, H₃-28), 0.86 (6H, s, H₃-18, H₃-19), 0.83 (3H, d, *J* = 6.6 Hz, H₃-26), 0.82 (3H, d, *J* = 6.6 Hz, H₃-27).

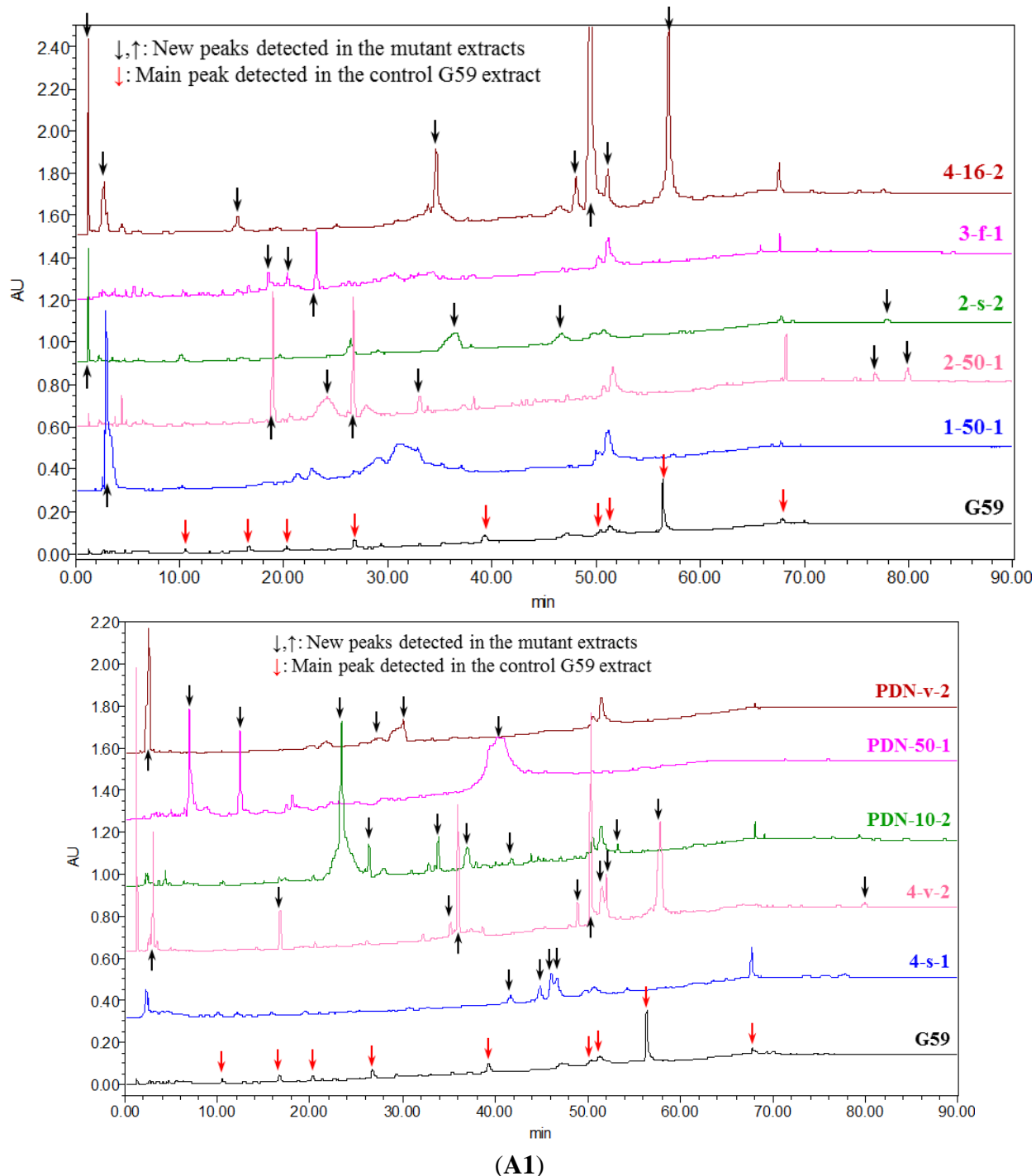
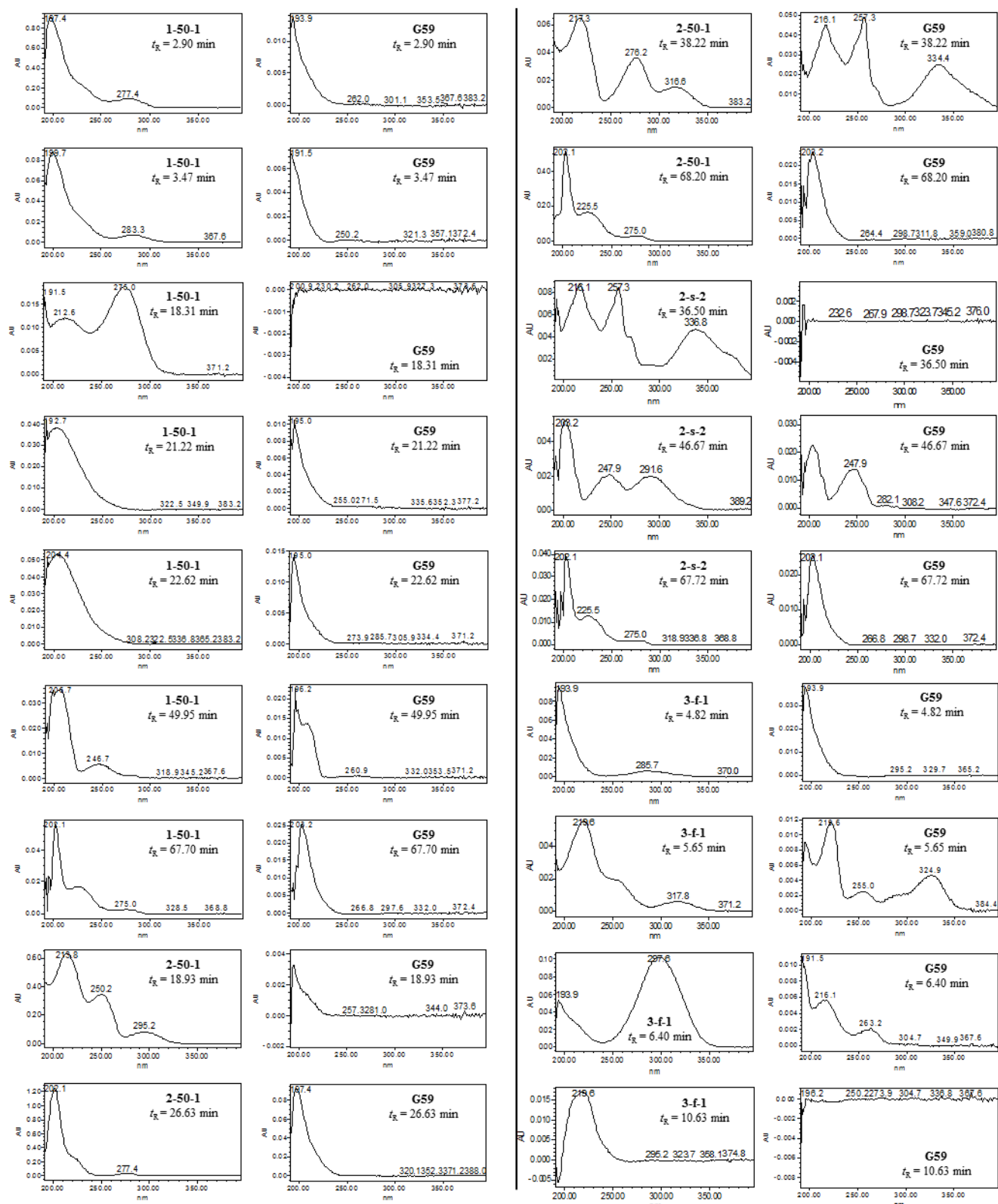
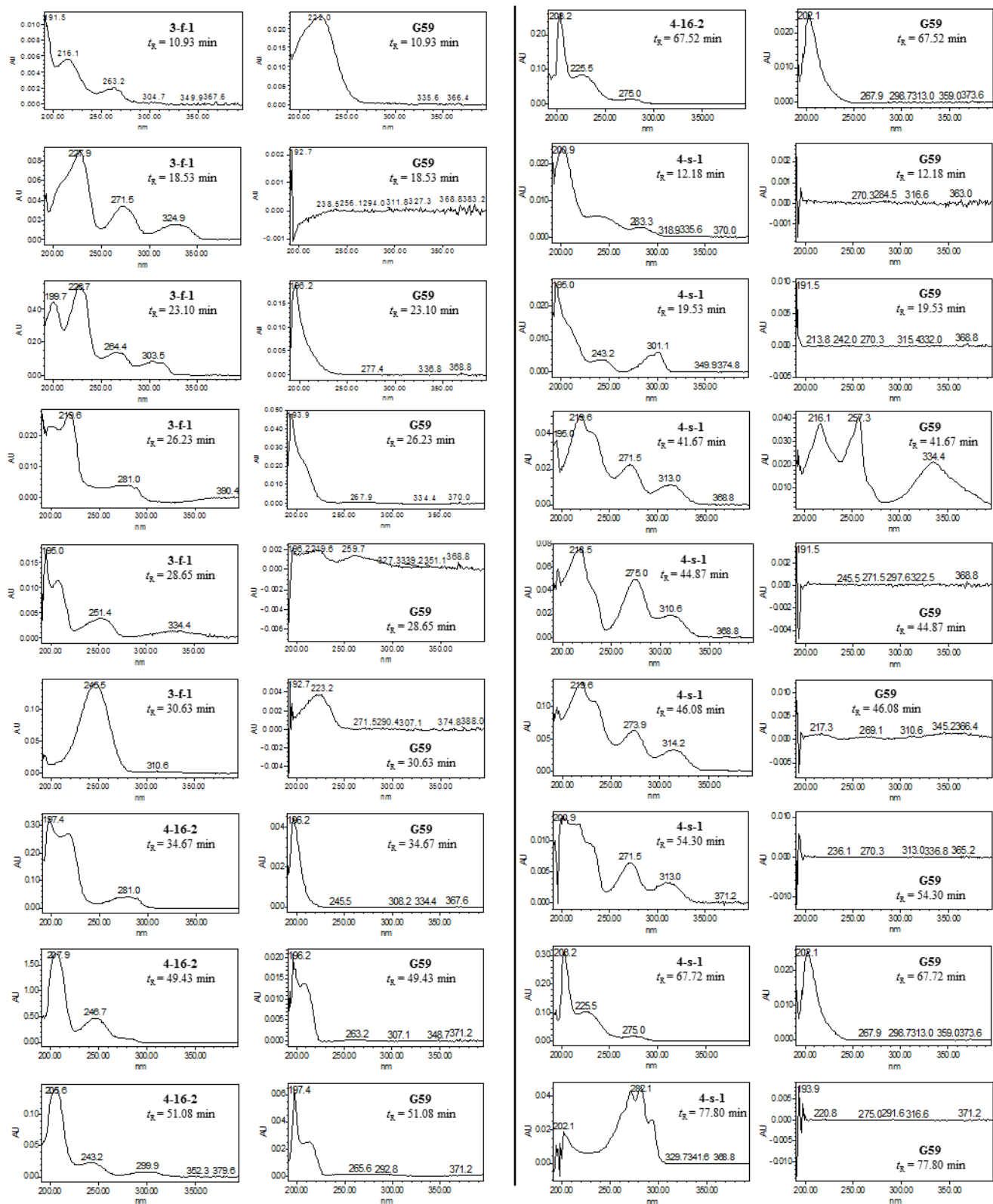


Figure S1. Cont.



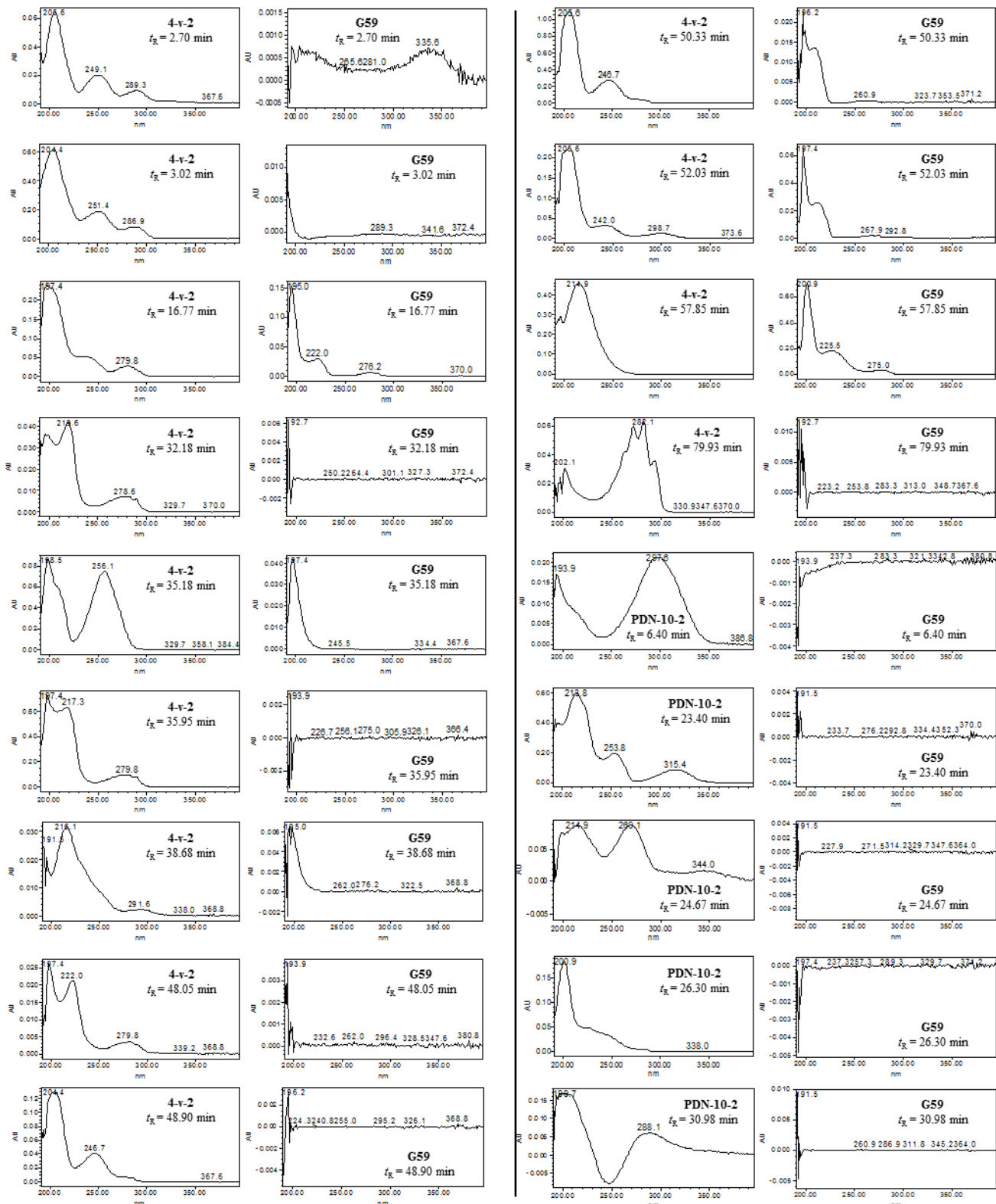
(A2)

Figure S1. Cont.



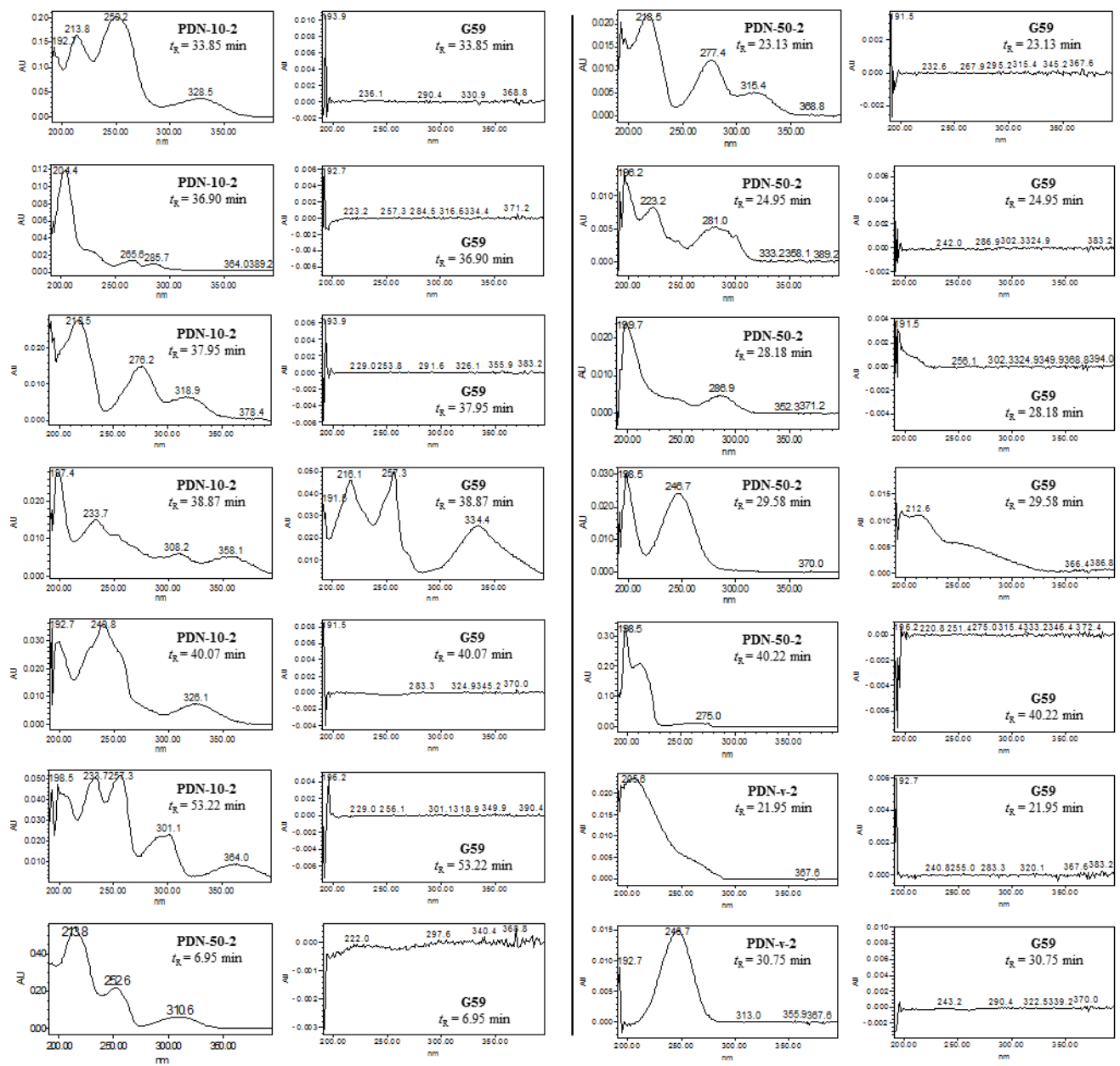
(A2)

Figure S1. Cont.



(A2)

Figure S1. Cont.



(A2)

Figure S1. Cont.

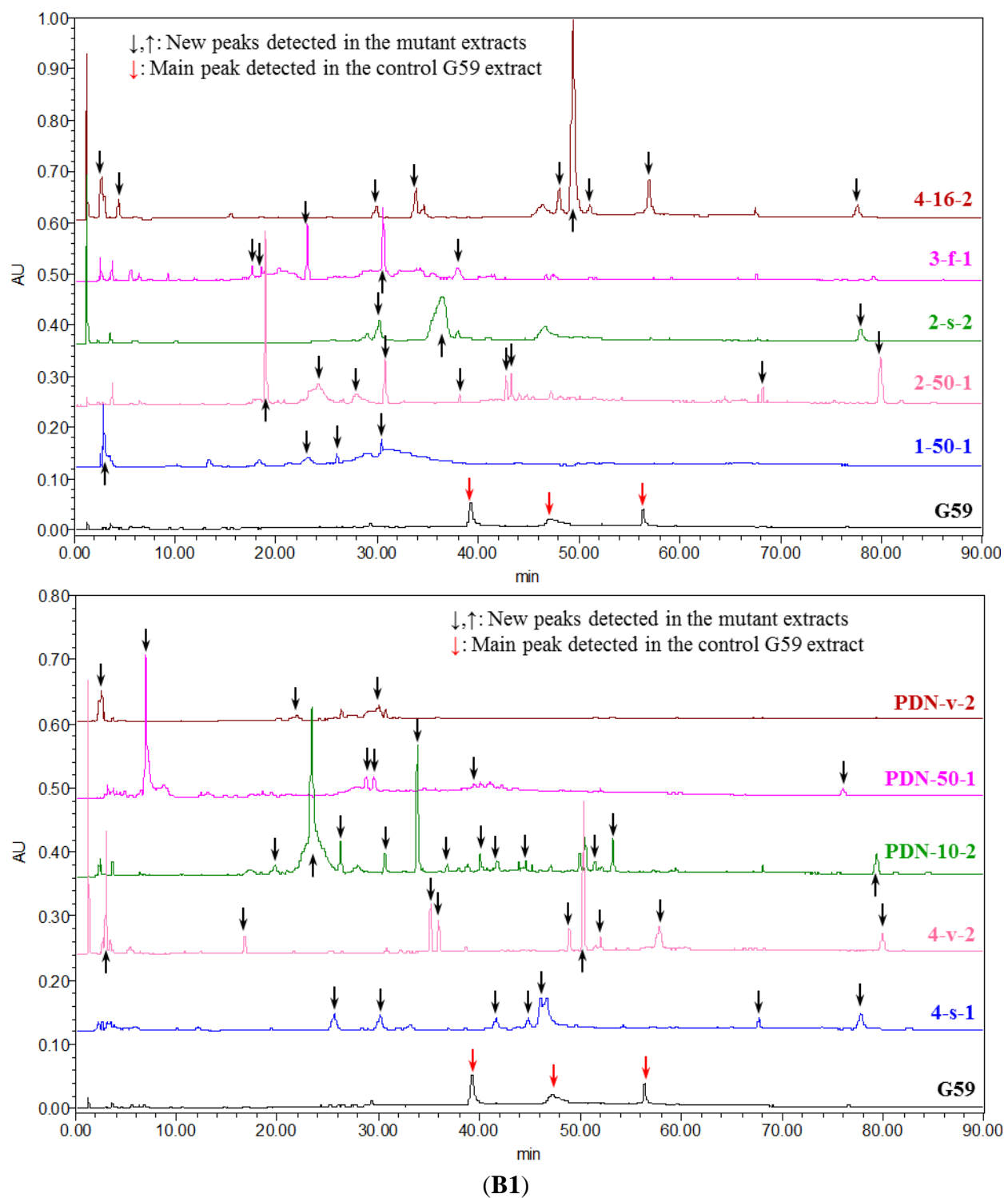
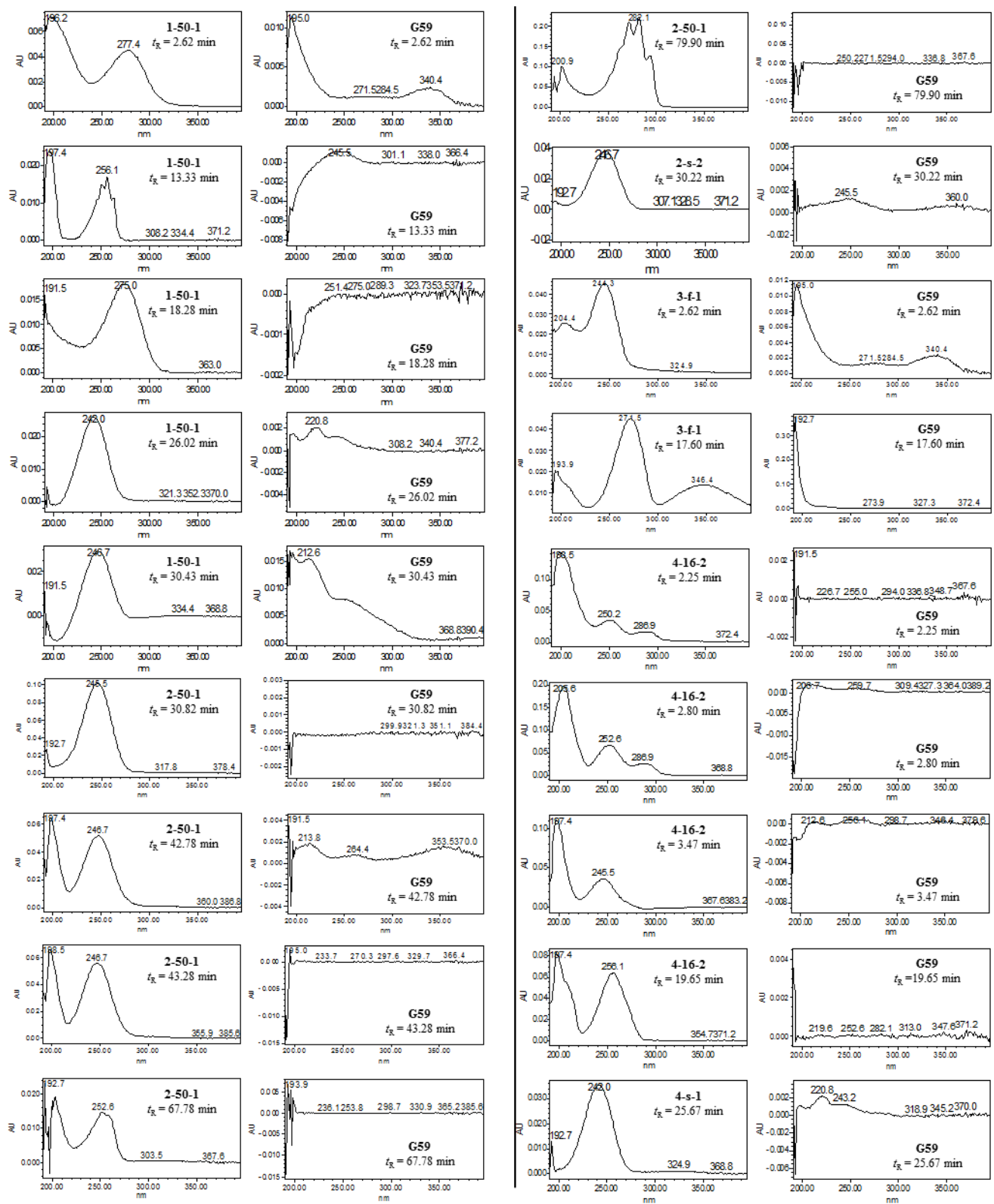
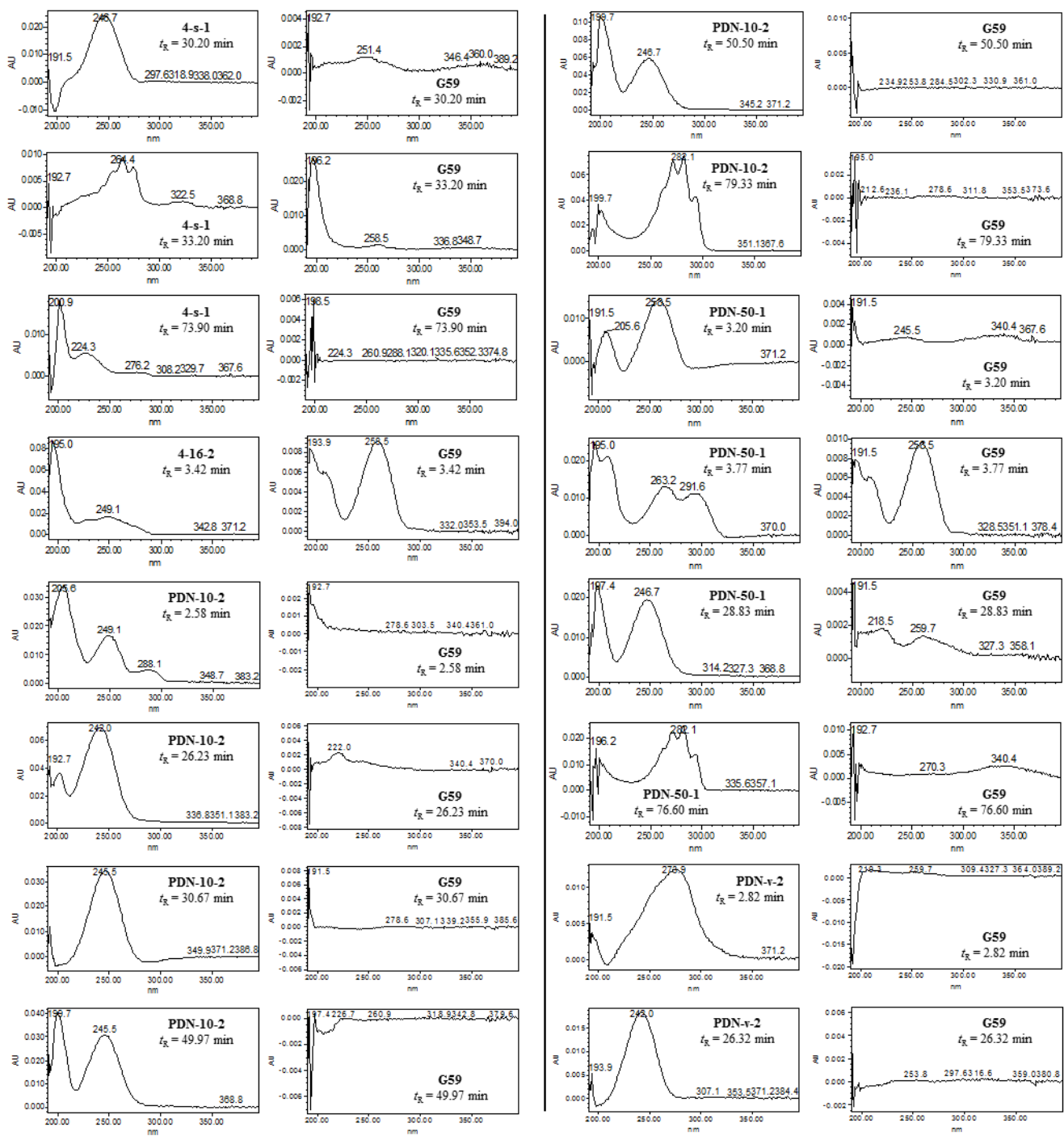


Figure S1. *Cont.*



(B2)

Figure S1. Cont.



(B2)

Figure S1. Cont.

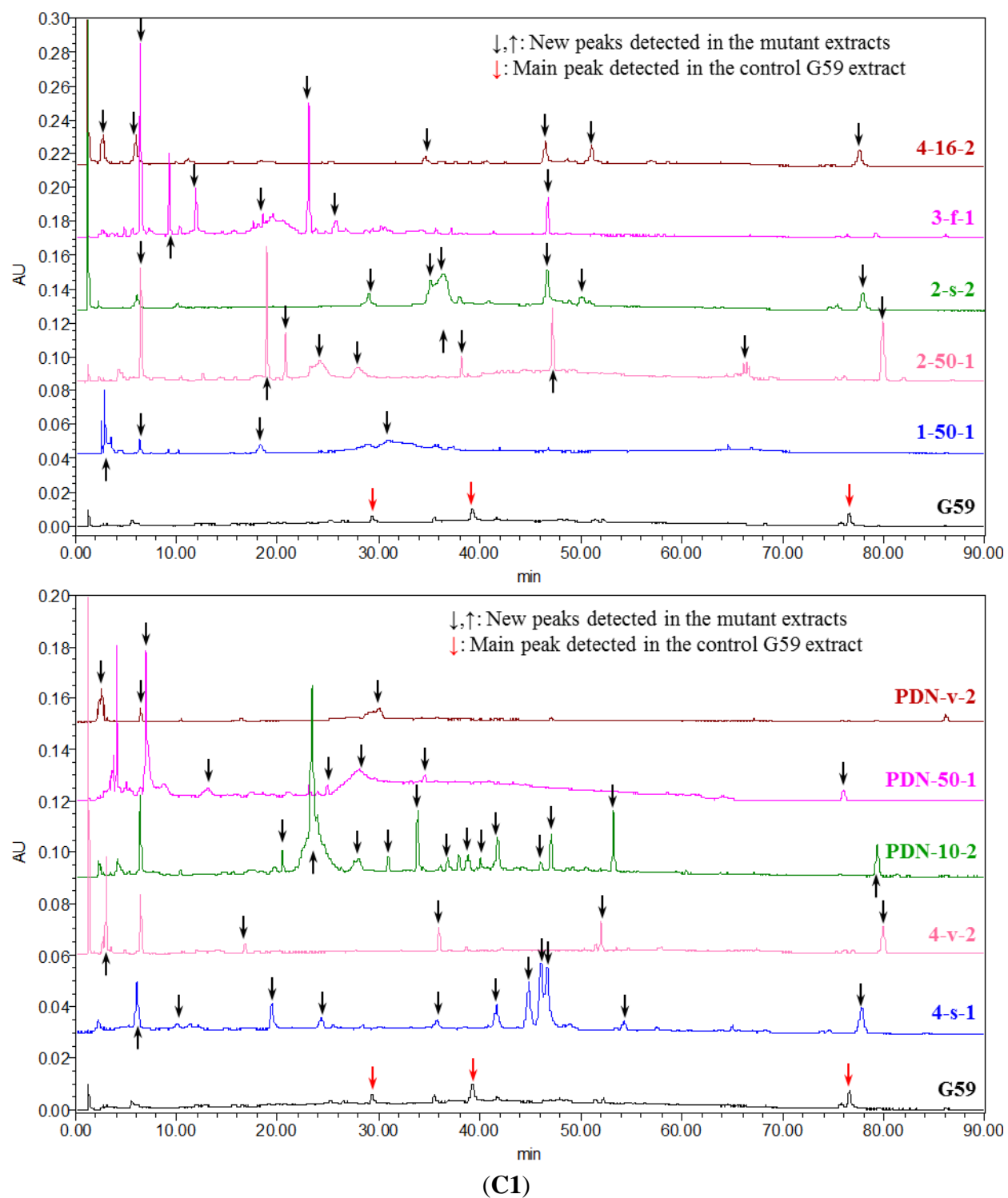
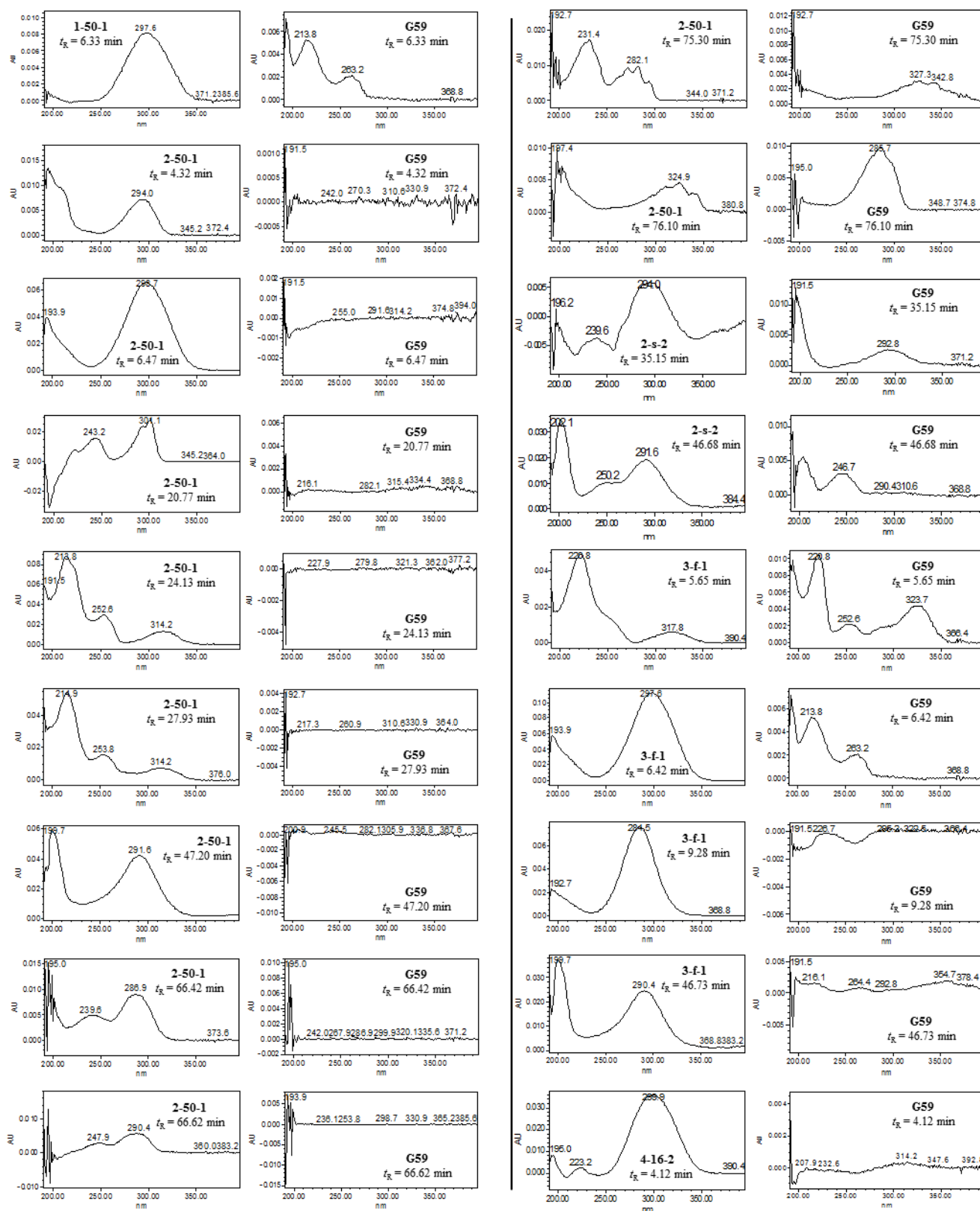
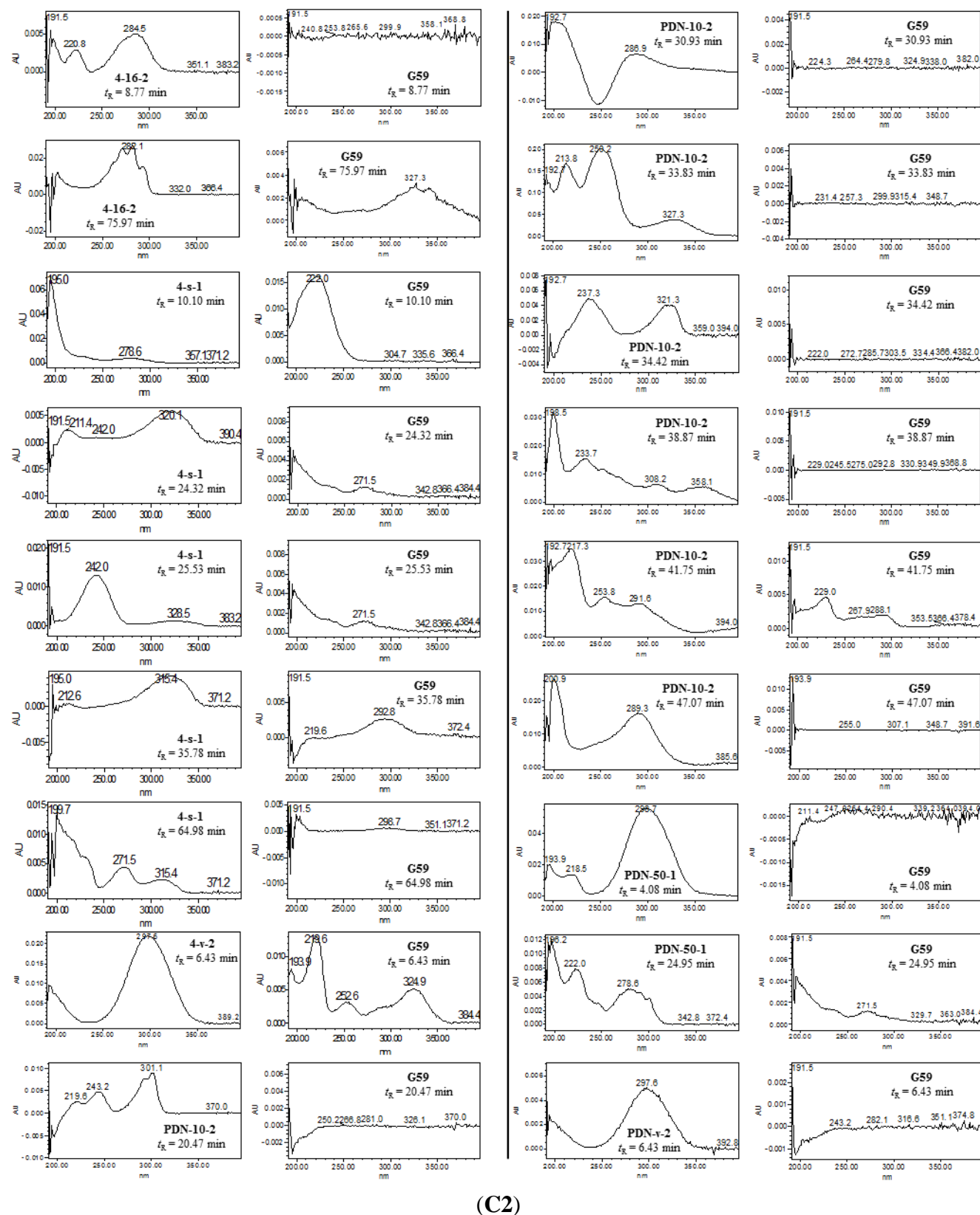


Figure S1. Cont.



(C2)

Figure S1. Cont.



(C2)

Figure S1. Cont.

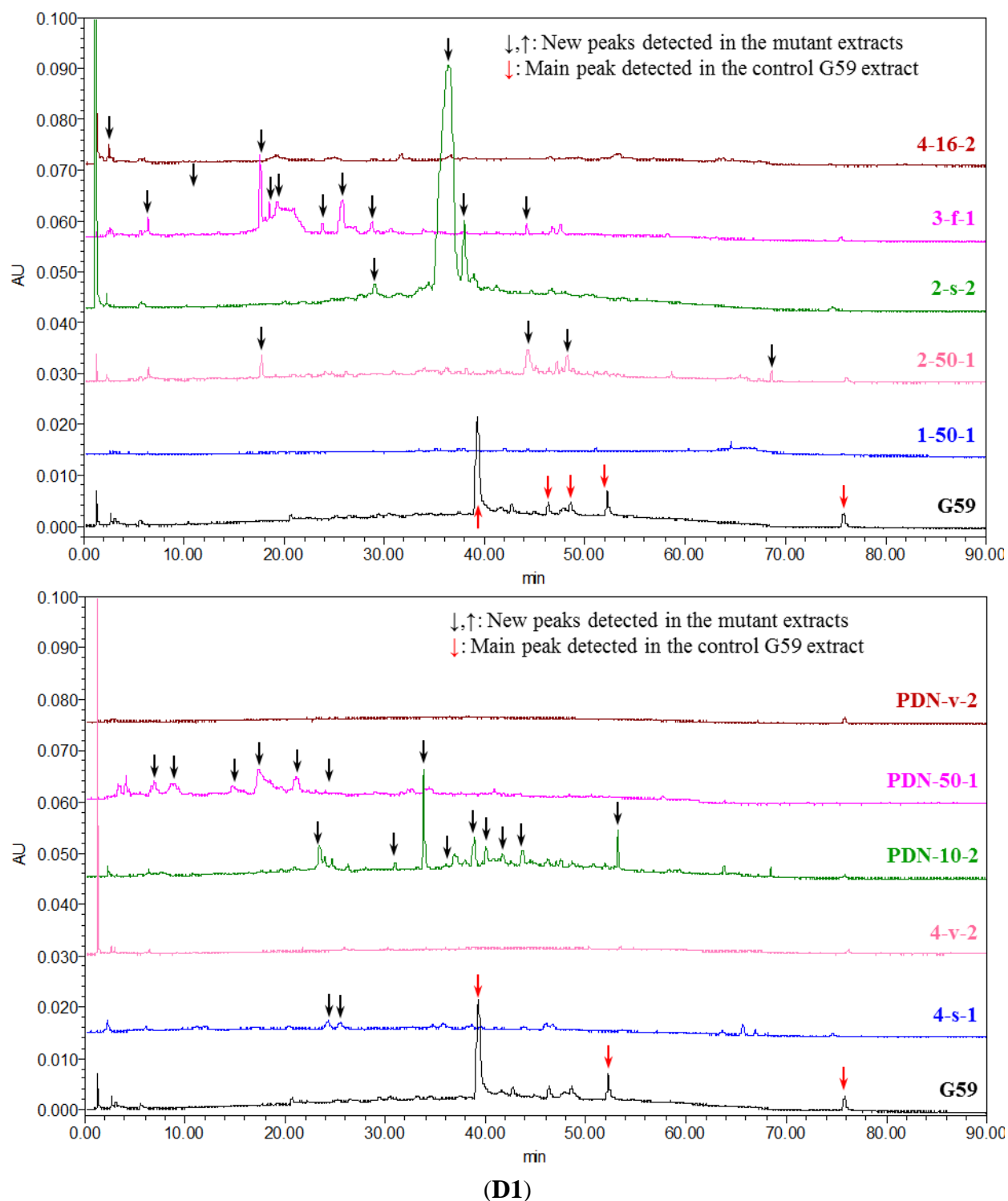
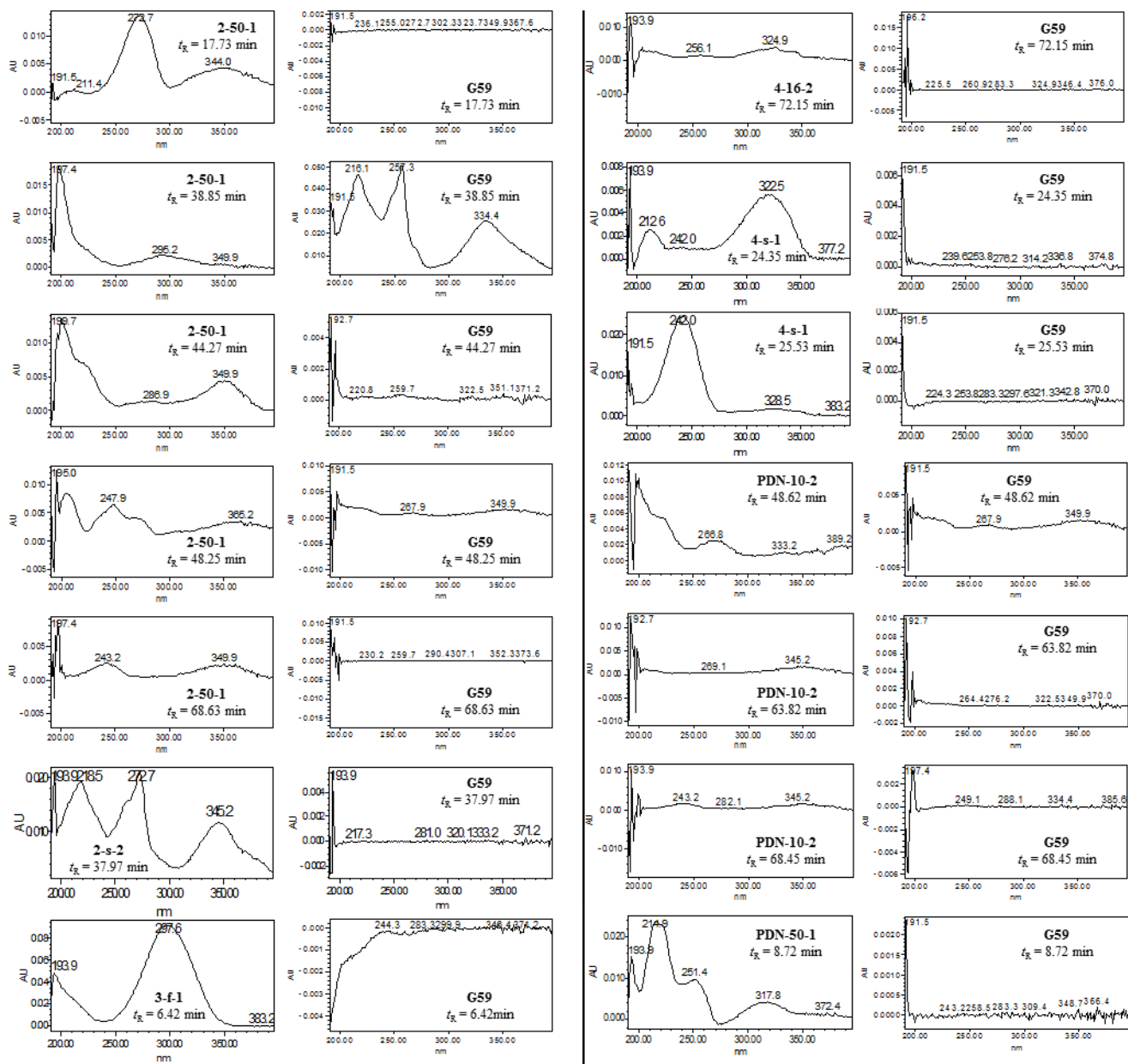
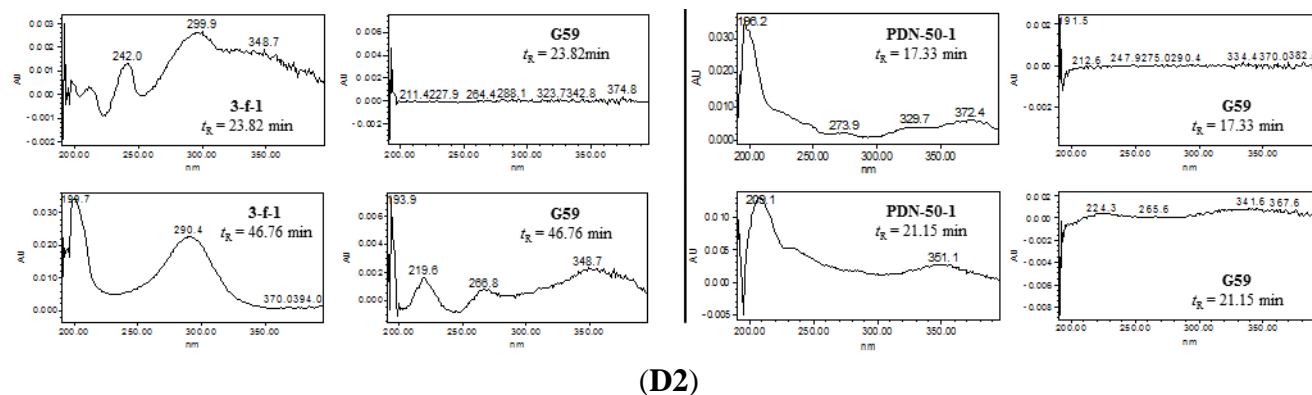


Figure S1. Cont.



(D2)

Figure S1. Cont.



(D2)

Figure S1. HPLC-PDAD-UV analysis of the EtOAc extracts of control G59 strain and its selected mutants. (A1) HPLC profiles detected at 210 nm; (A2) UV spectra of the new peaks in mutant extracts in the HPLC profiles at 210 nm, and UV absorptions of the control G59 extract at the corresponding retention times; (B1) HPLC profiles detected at 254 nm; (B2) UV spectra of the new peaks in mutant extracts in the HPLC profiles at 254 nm, and UV absorptions of the control G59 extract at the corresponding retention times; (C1) HPLC profiles detected at 300 nm; (C2) UV spectra of the new peaks in mutant extracts in the HPLC profiles at 300 nm, and UV absorptions of the control G59 extract at the corresponding retention times; (D1) HPLC profiles detected at 350 nm; (D2) UV spectra of the new peaks in mutant extracts in the HPLC profiles at 350 nm, and UV absorptions of the control G59 extract at the corresponding retention times.

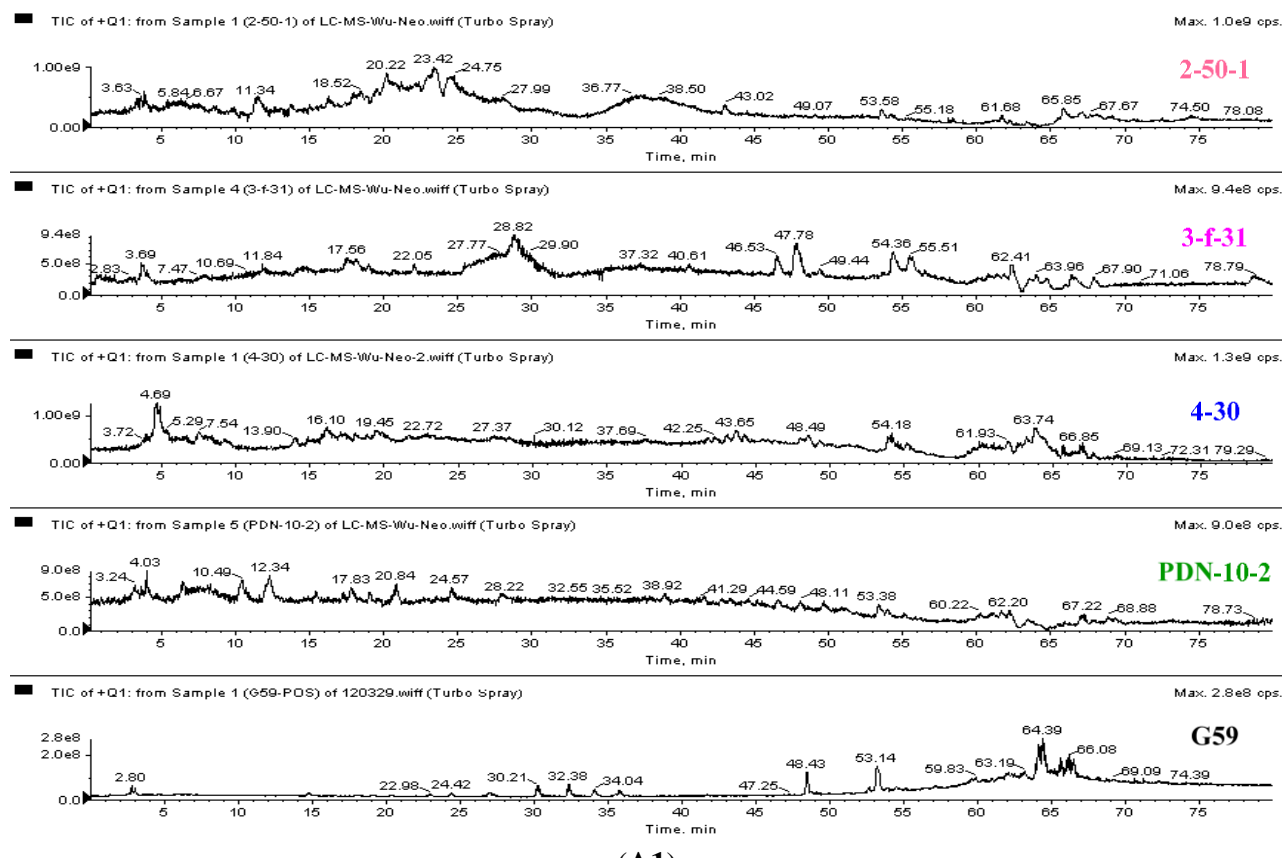
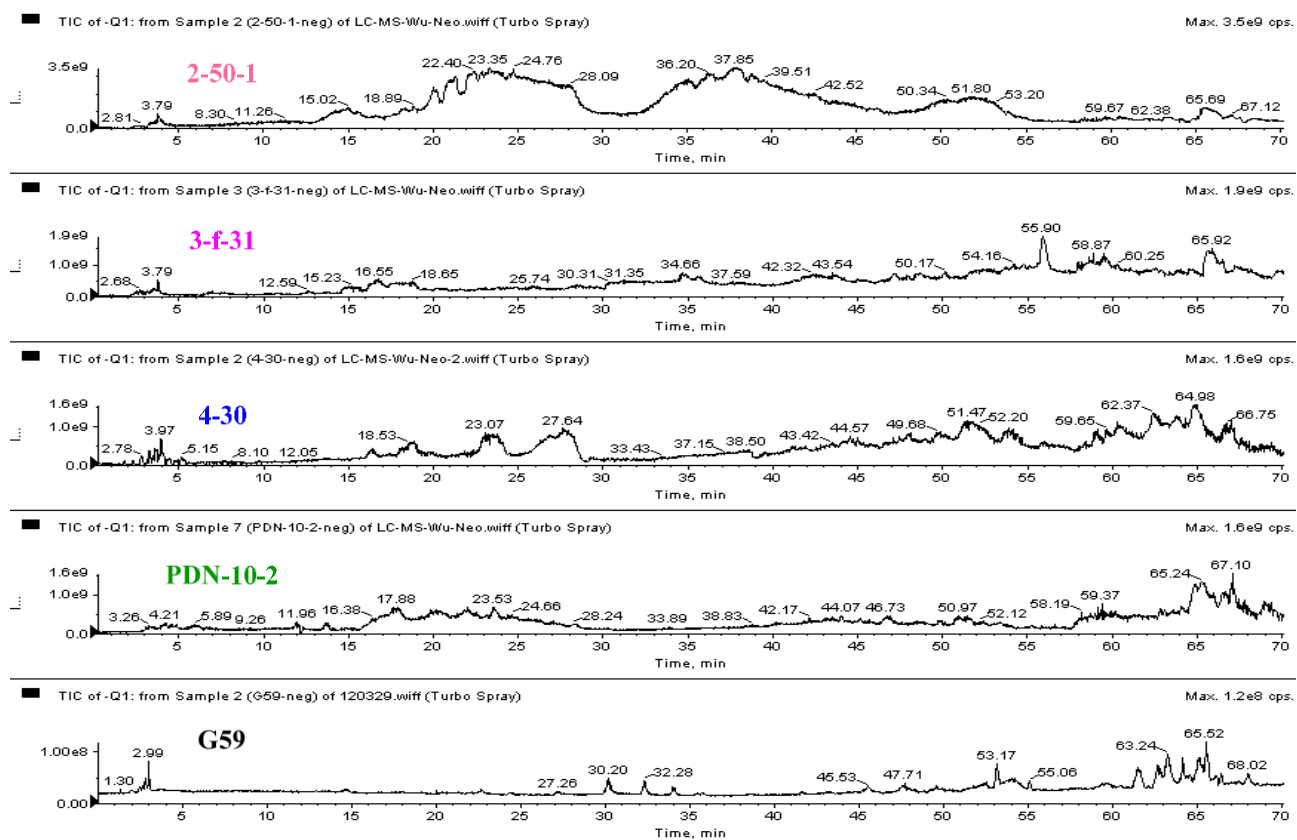
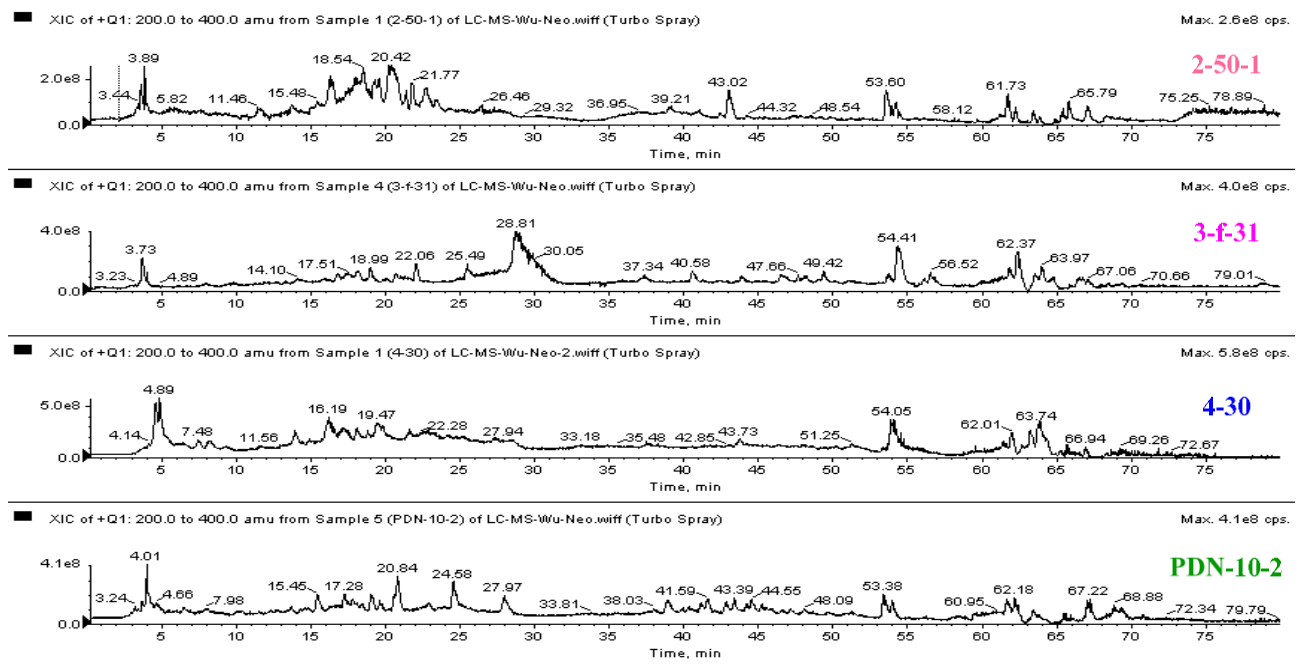


Figure S2. Cont.



(A2)



(B1)

Figure S2. Cont.

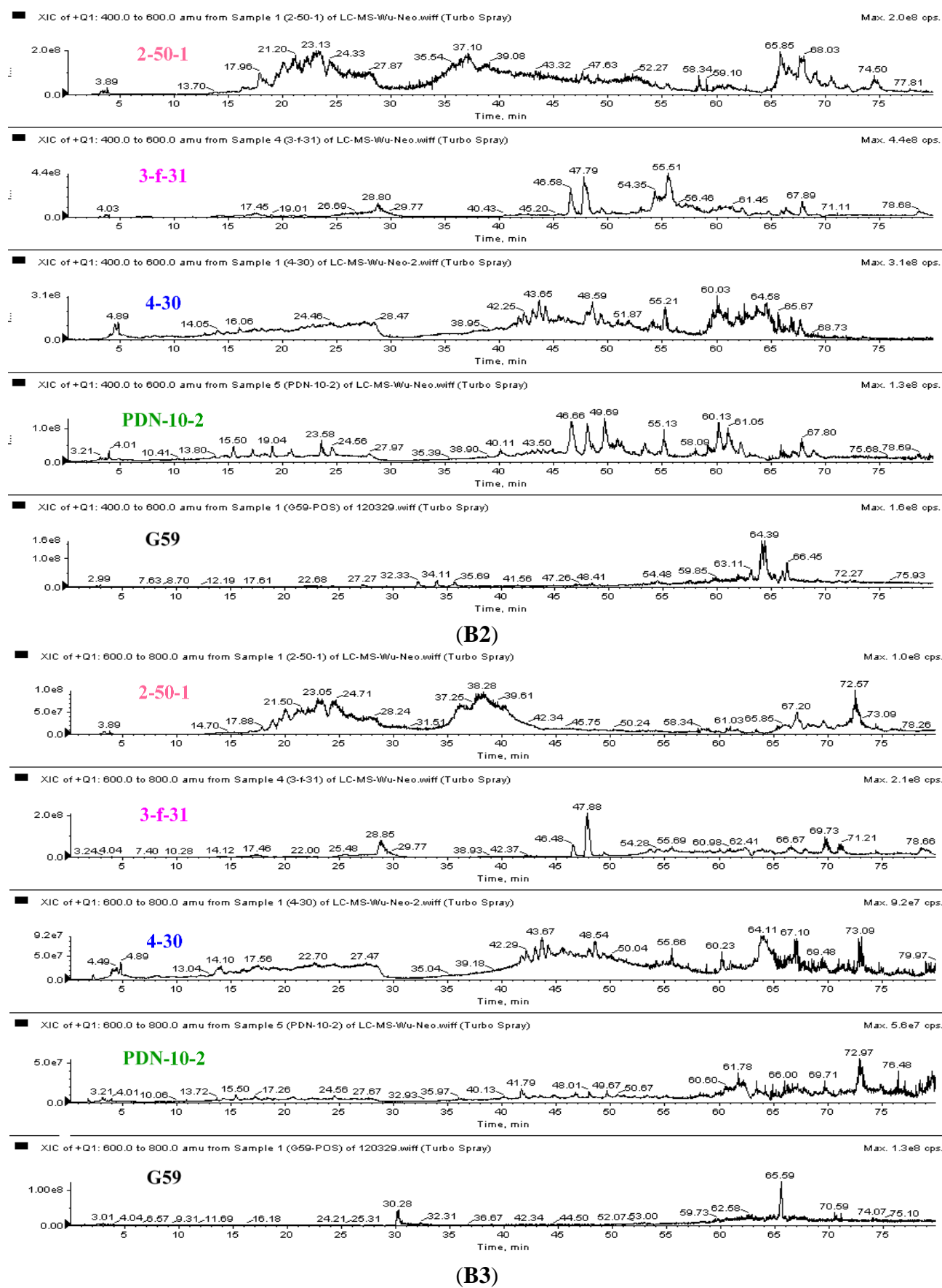


Figure S2. Cont.

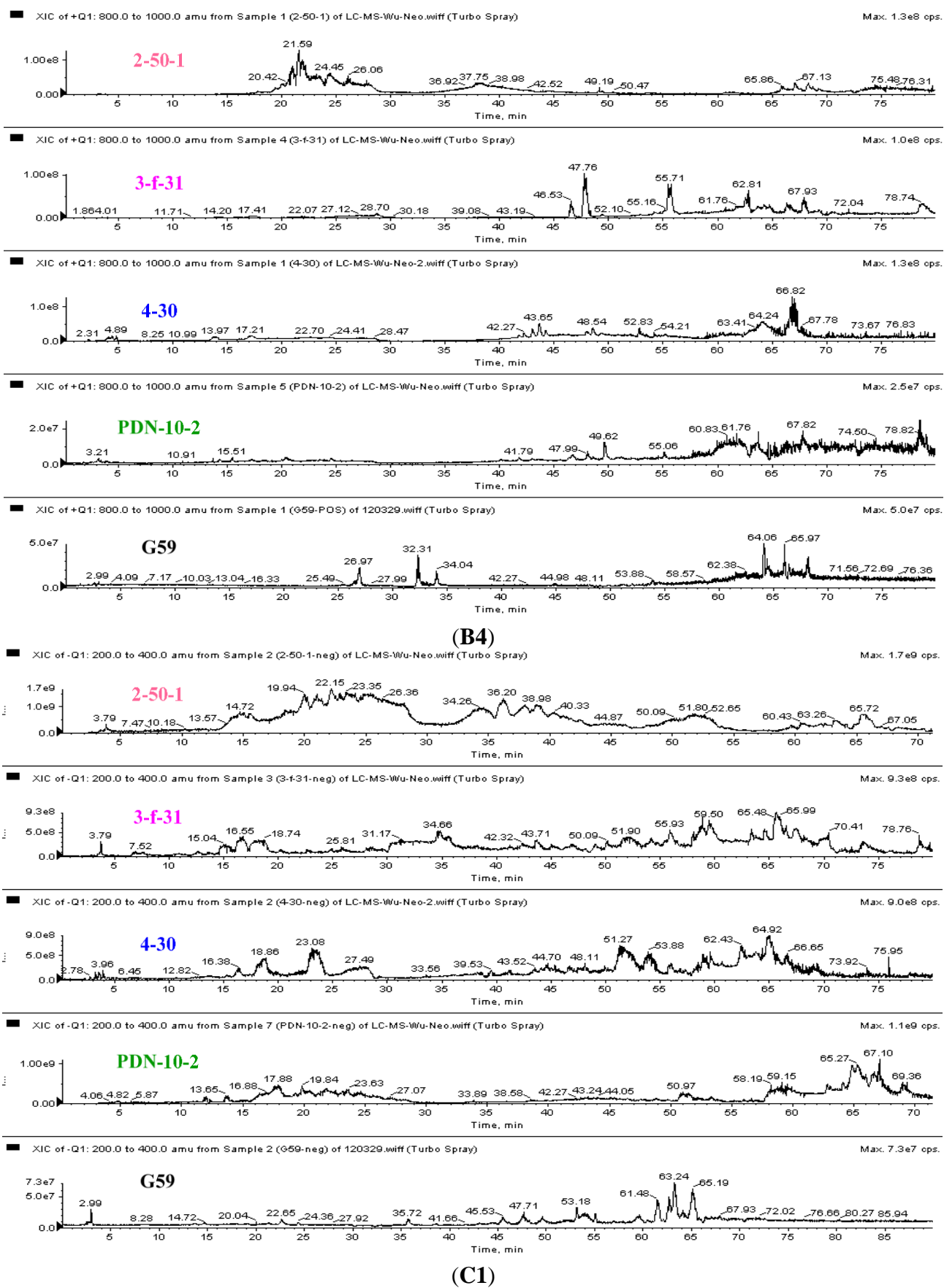


Figure S2. Cont.

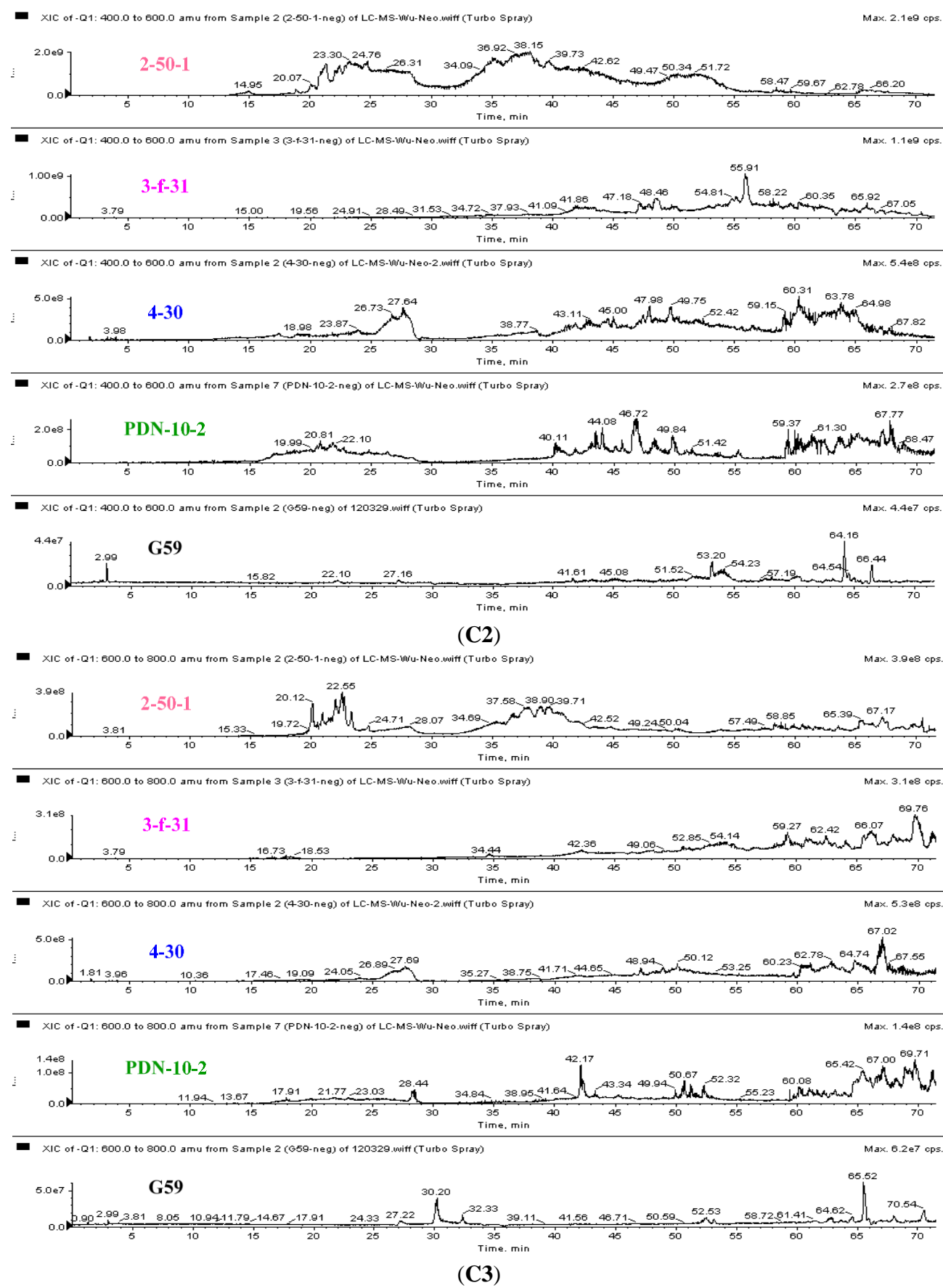


Figure S2. Cont.

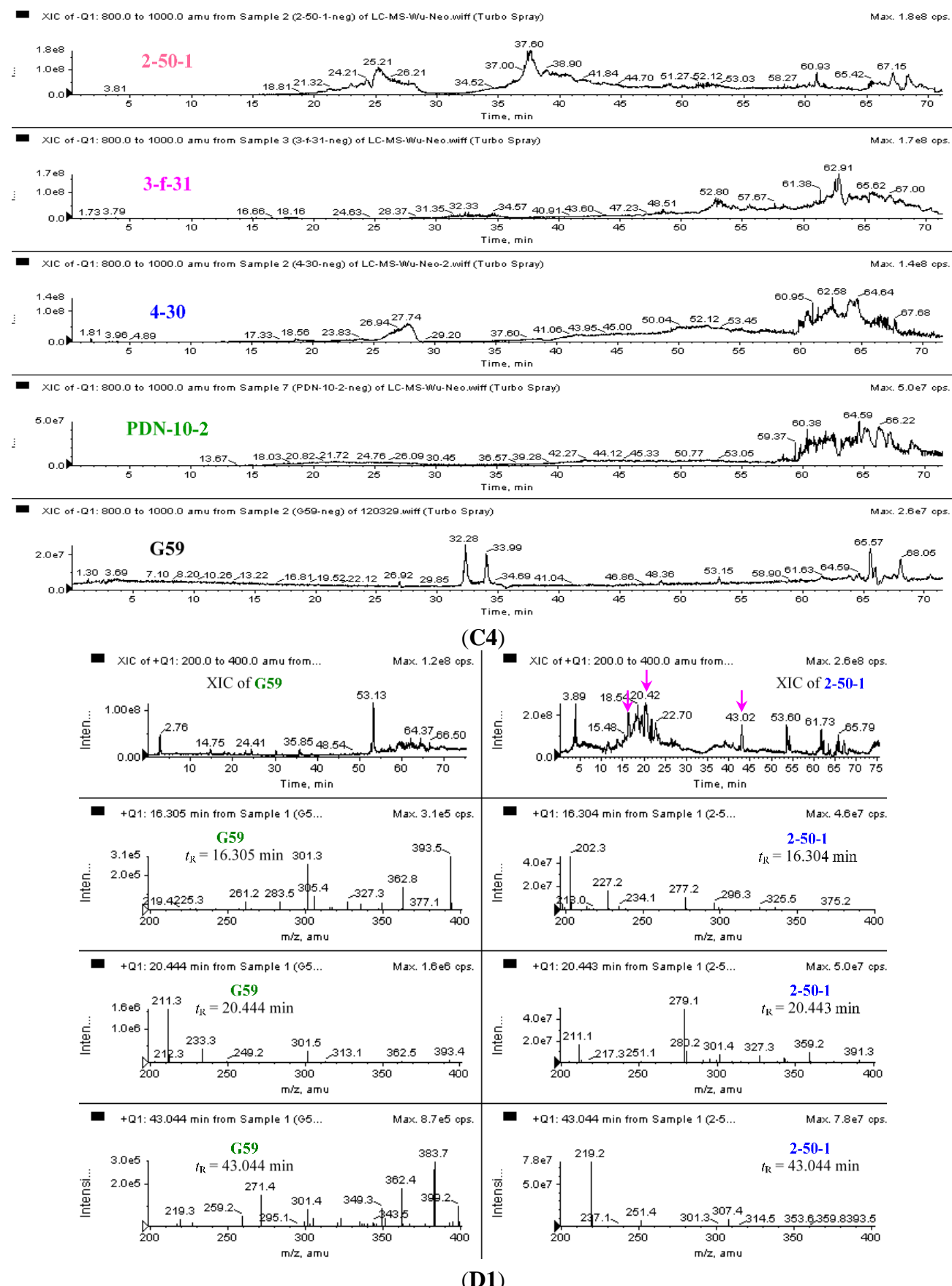


Figure S2. *Cont.*

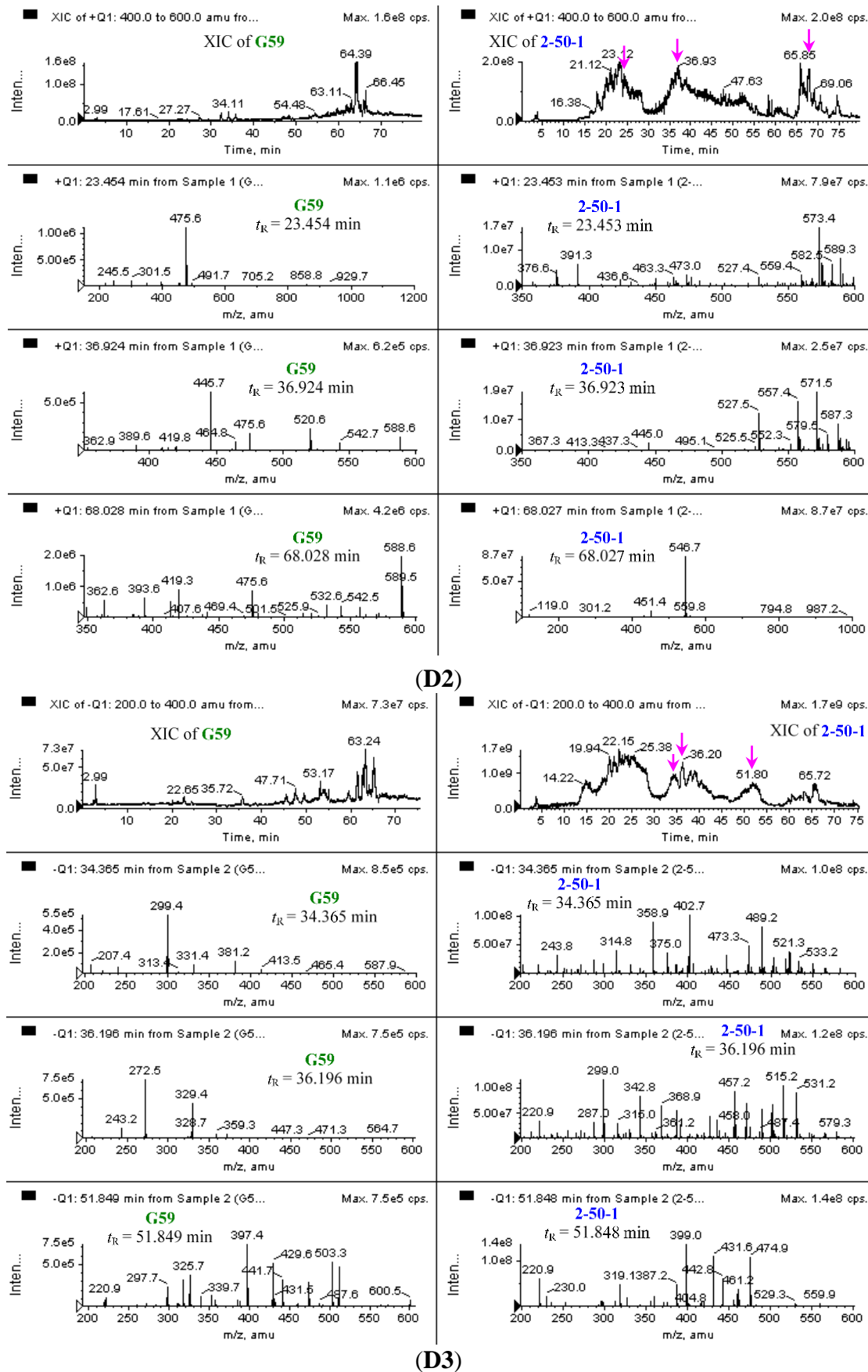


Figure S2. Cont.

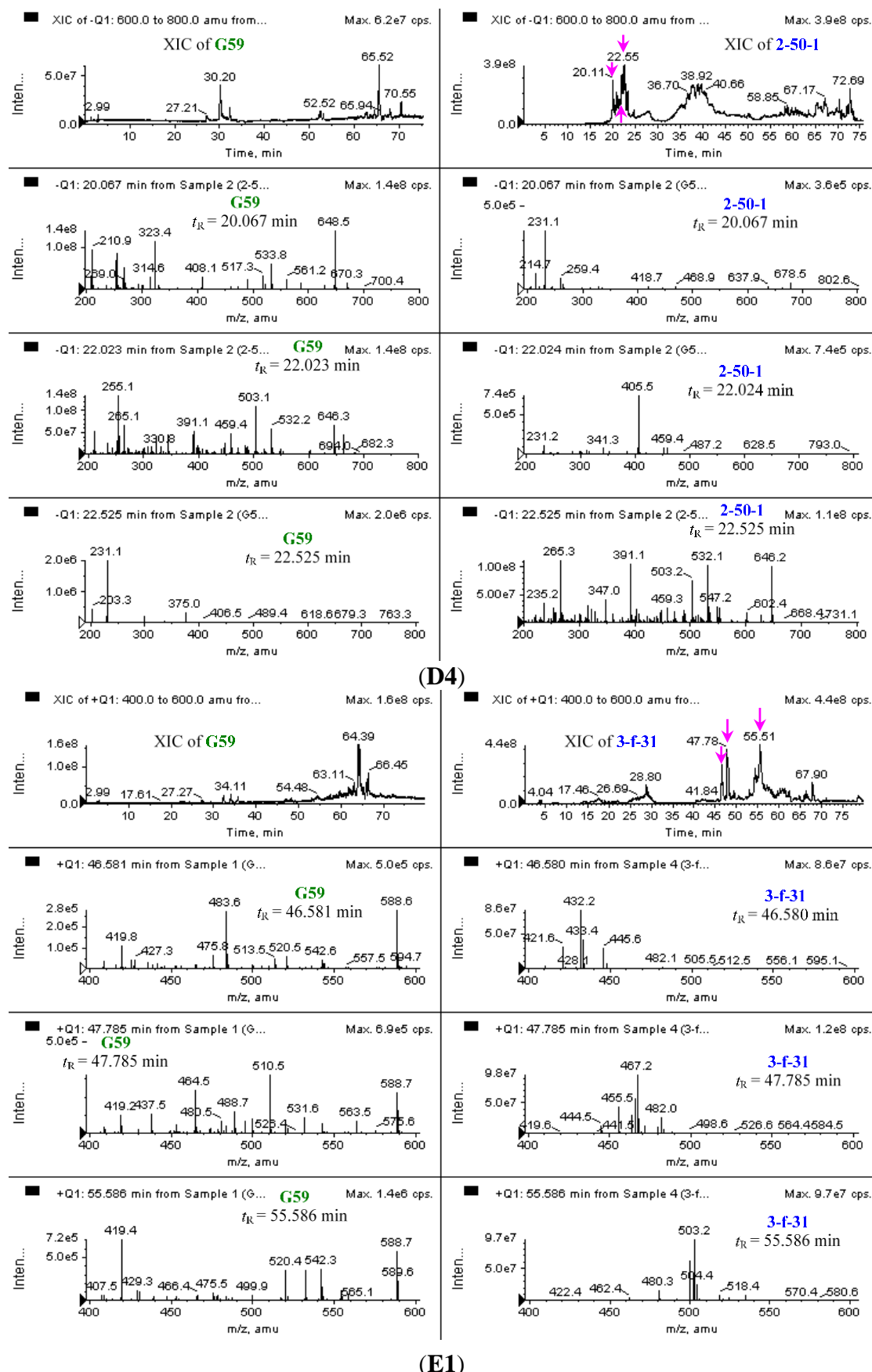


Figure S2. Cont.

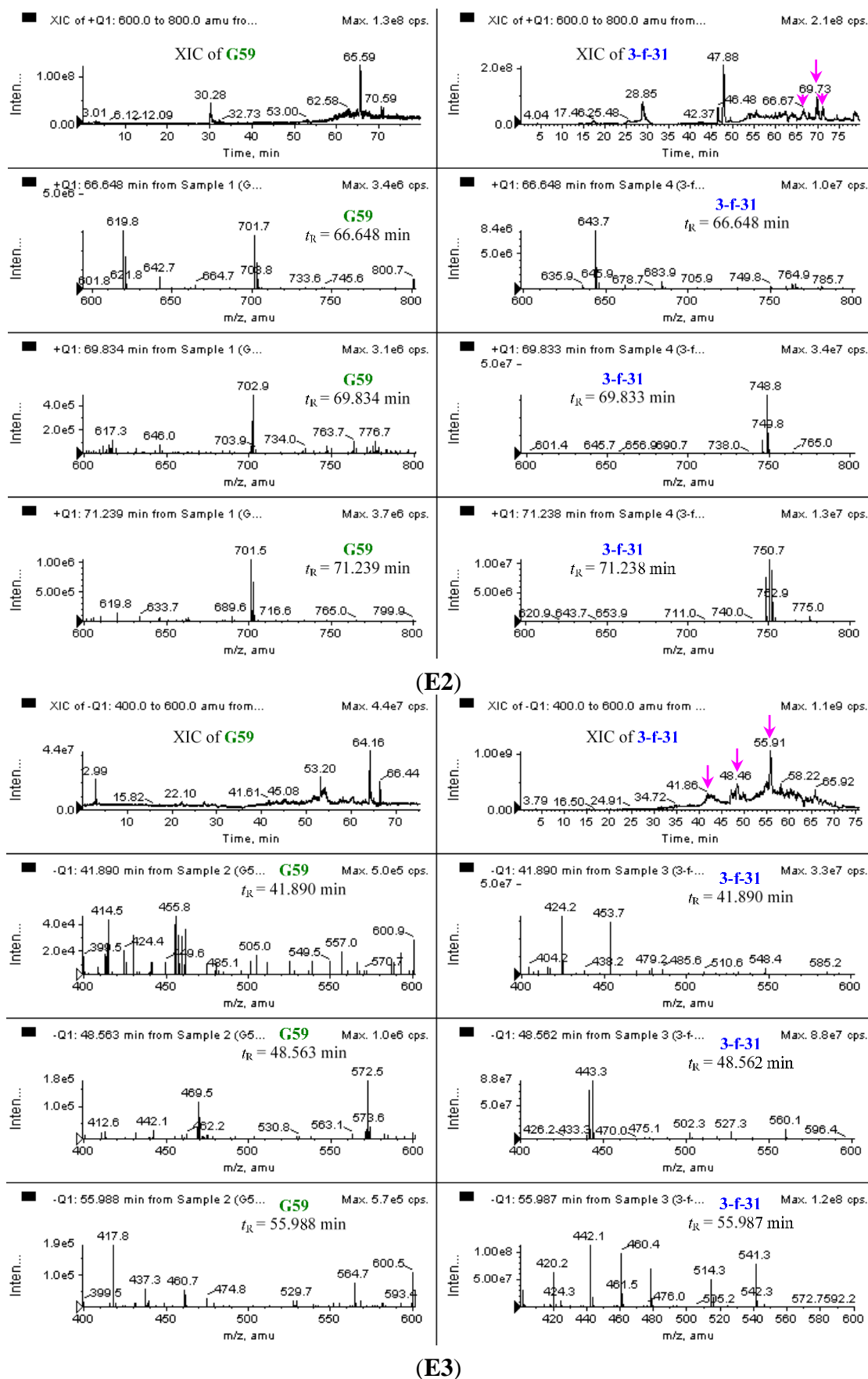


Figure S2. Cont.

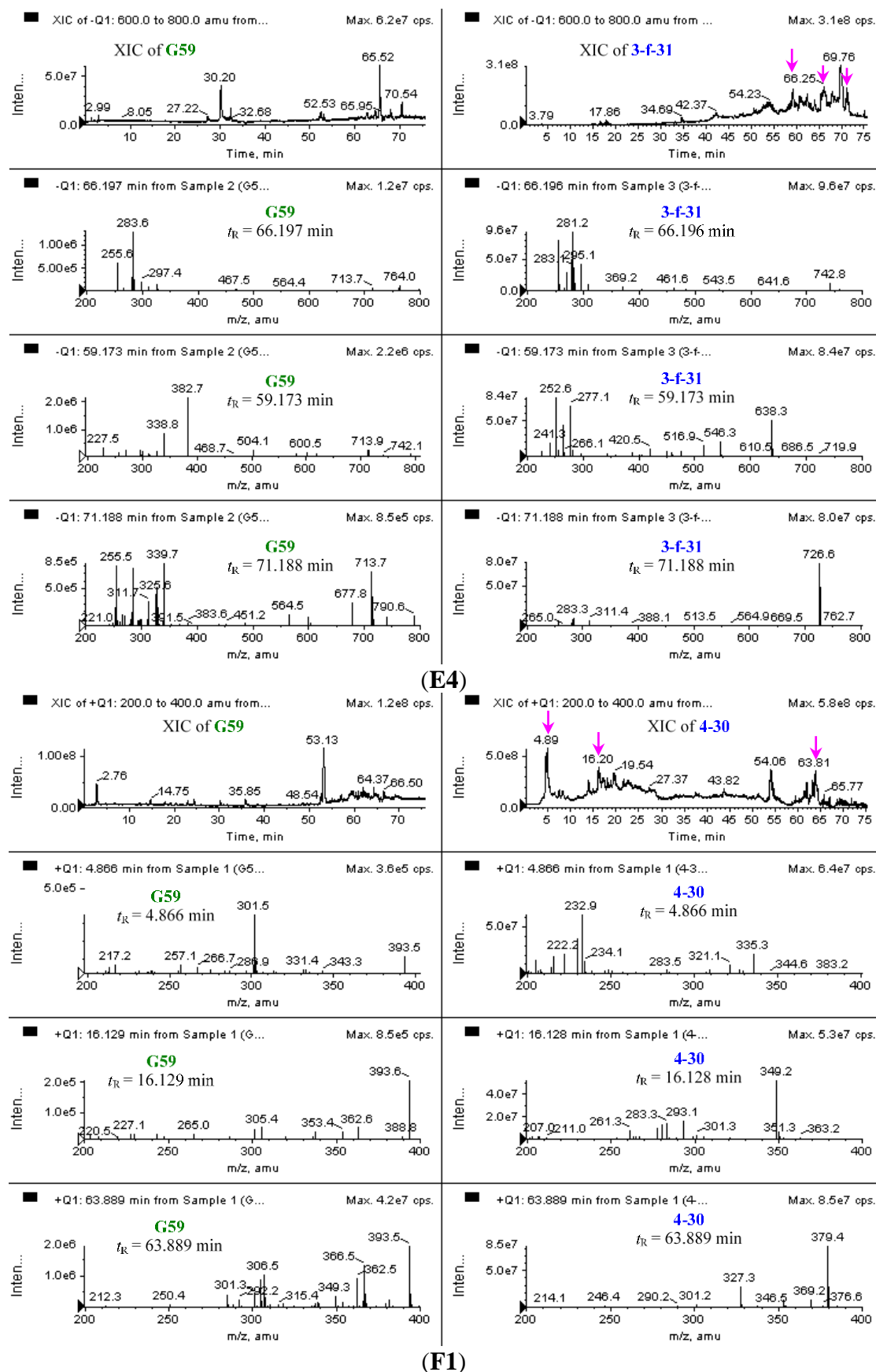


Figure S2. Cont.

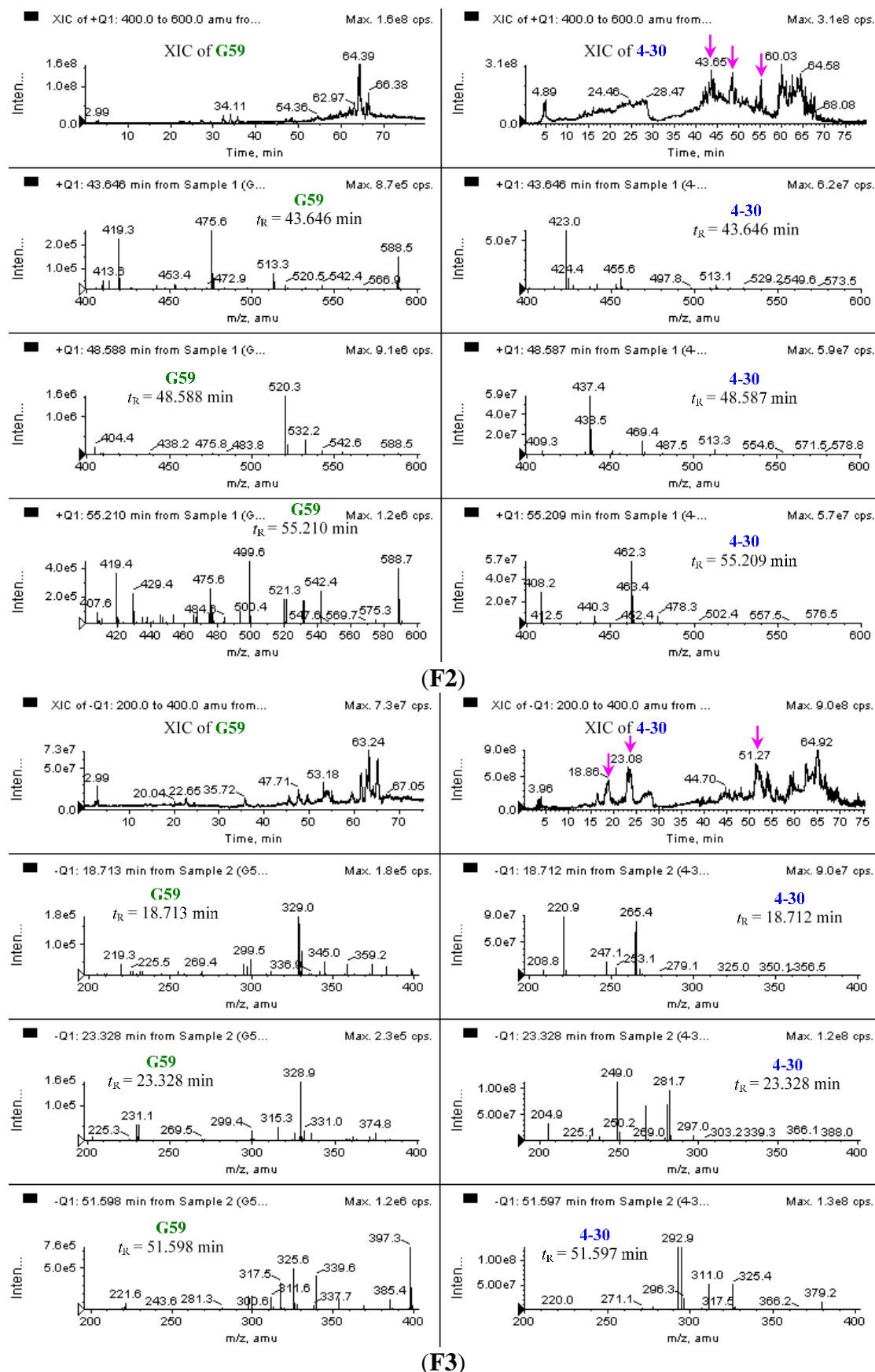


Figure S2. Cont.

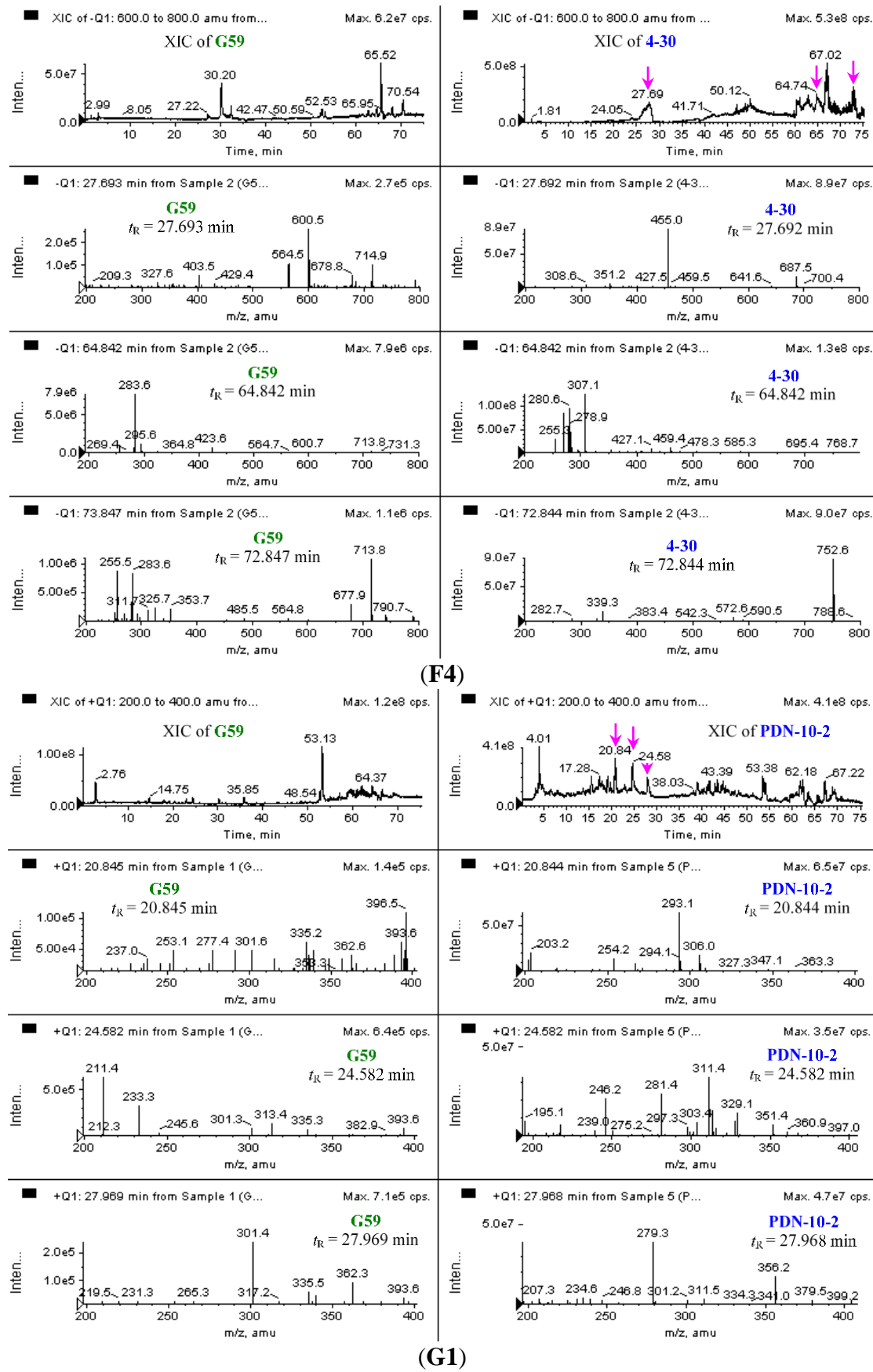


Figure S2. Cont.

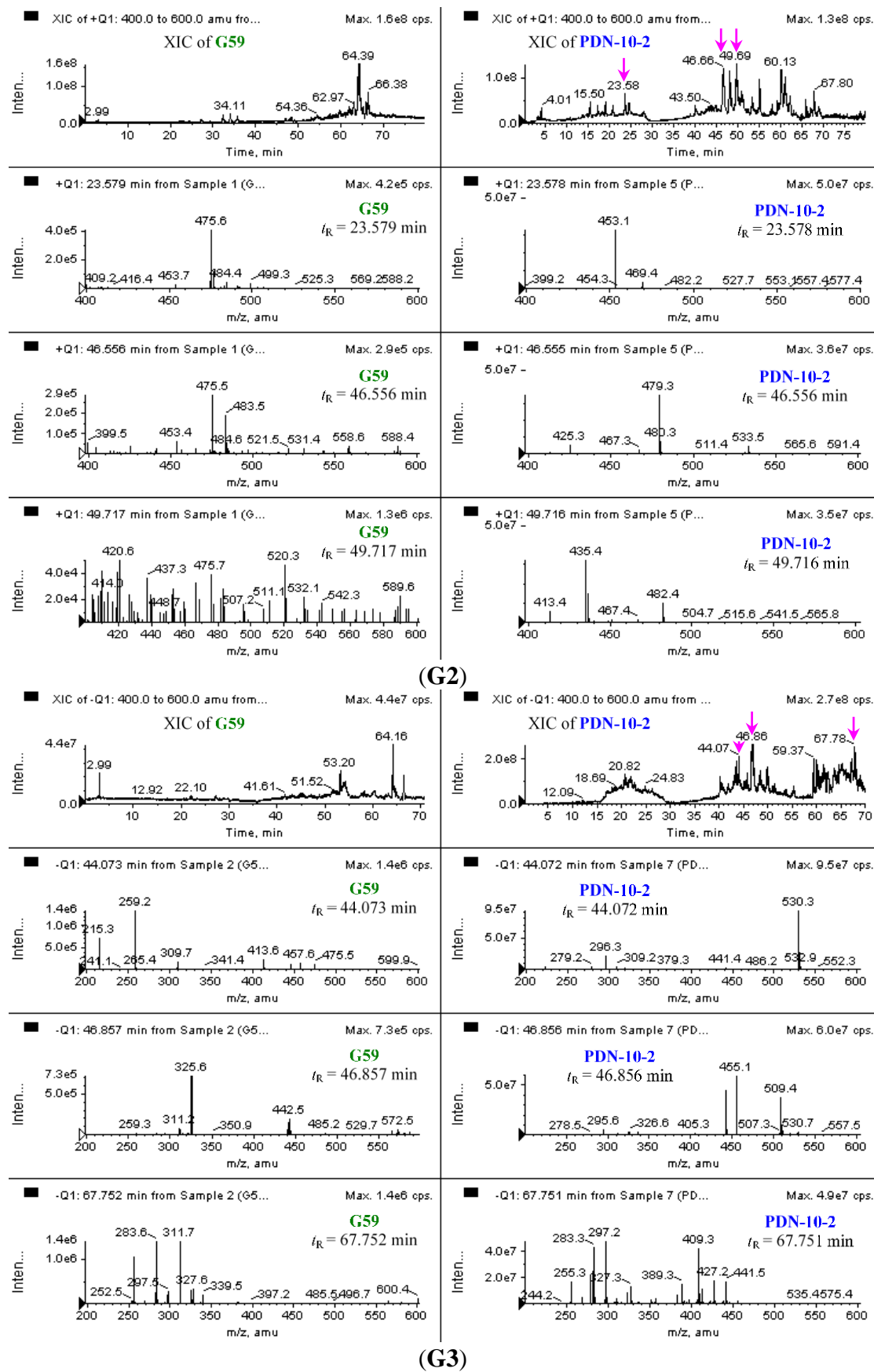
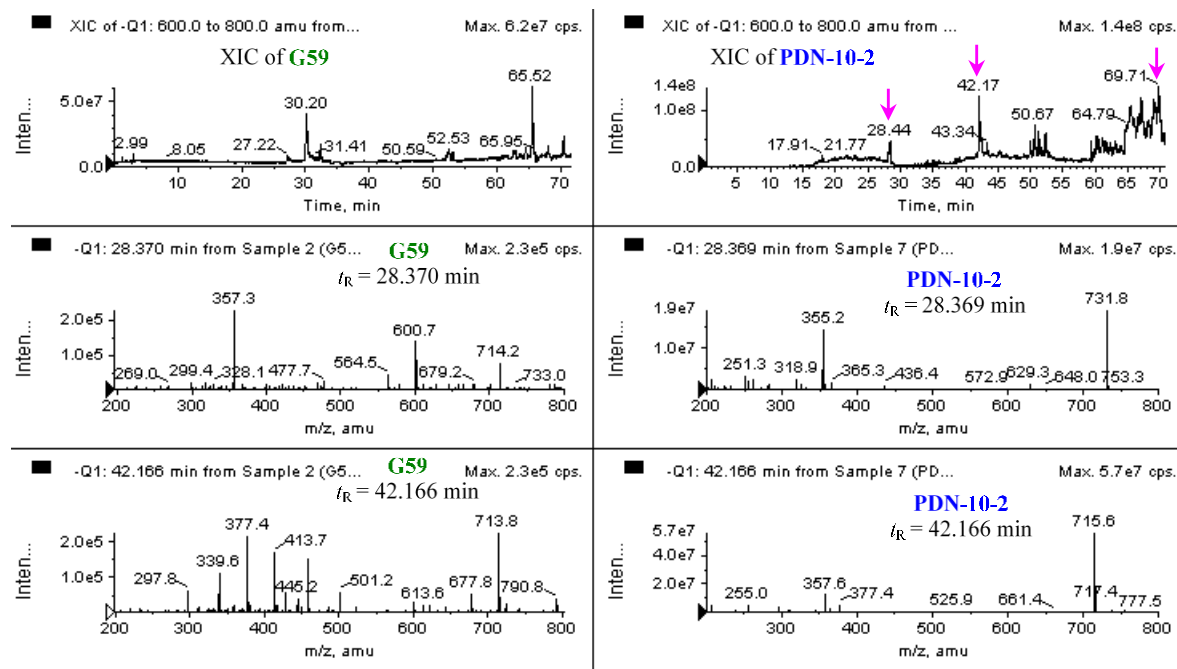


Figure S2. Cont.



(G4)

Figure S2. Cont.

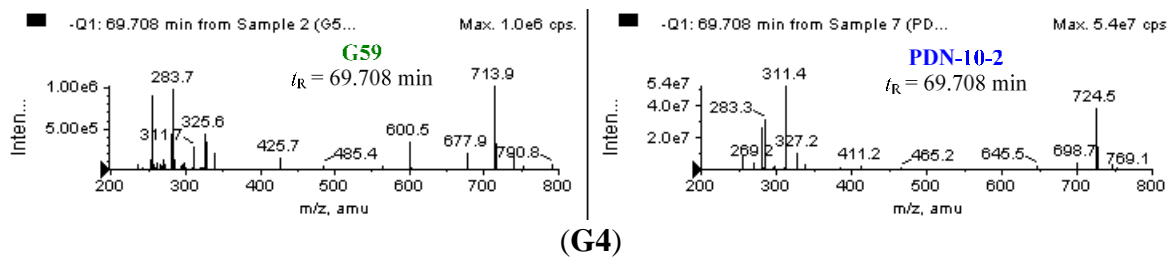


Figure S2. HPLC-ESI-MS analysis of the EtOAc extracts of control G59 strain and its selected mutants. **(A1)** Positive total ion chromatograms; **(A2)** Negative total ion chromatograms; **(B1)** Positive extracted ion chromatograms (XICs) (200–400 m/z); **(B2)** Positive extracted ion chromatograms (XICs) (400–600 m/z); **(B3)** Positive extracted ion chromatograms (XICs) (600–800 m/z); **(B4)** Positive extracted ion chromatograms (XICs) (800–1000 m/z); **(C1)** Negative extracted ion chromatograms (XICs) (200–400 m/z); **(C2)** Negative extracted ion chromatograms (XICs) (400–600 m/z); **(C3)** Negative extracted ion chromatograms (XICs) (600–800 m/z); **(C4)** Negative extracted ion chromatograms (XICs) (800–1000 m/z); **(D1)** MS spectra extracted from the positive XICs (200–400 m/z) of control G59 and mutant 2-50-1; **(D2)** MS spectra extracted from the positive XICs (400–600 m/z) of control G59 and mutant 2-50-1; **(D3)** MS spectra extracted from the negative XICs (200–400 m/z) of control G59 and mutant 2-50-1; **(D4)** MS spectra extracted from the negative XICs (600–800 m/z) of control G59 and mutant 2-50-1; **(E1)** MS spectra extracted from the positive XICs (400–600 m/z) of control G59 and mutant 3-f-31; **(E2)** MS spectra extracted from the positive XICs (600–800 m/z) of control G59 and mutant 3-f-31; **(E3)** MS spectra extracted from the negative XICs (400–600 m/z) of control G59 and mutant 3-f-31; **(E4)** MS spectra extracted from the negative XICs (600–800 m/z) of control G59 and mutant 3-f-31; **(F1)** MS spectra extracted from the positive XICs (200–400 m/z) of control G59 and mutant 4-30; **(F2)** MS spectra extracted from the positive XICs (400–600 m/z) of control G59 and mutant 4-30; **(F3)** MS spectra extracted from the negative XICs (200–400 m/z) of control G59 and mutant 4-30; **(F4)** MS spectra extracted from the negative XICs (600–800 m/z) of control G59 and mutant 4-30; **(G1)** MS spectra extracted from the positive XICs (200–400 m/z) of control G59 and mutant PDN-10-2; **(G2)** MS spectra extracted from the positive XICs (400–600 m/z) of control G59 and mutant PDN-10-2; **(G3)** MS spectra extracted from the negative XICs (400–600 m/z) of control G59 and mutant PDN-10-2; **(G4)** MS spectra extracted from the negative XICs (600–800 m/z) of control G59 and mutant PDN-10-2.

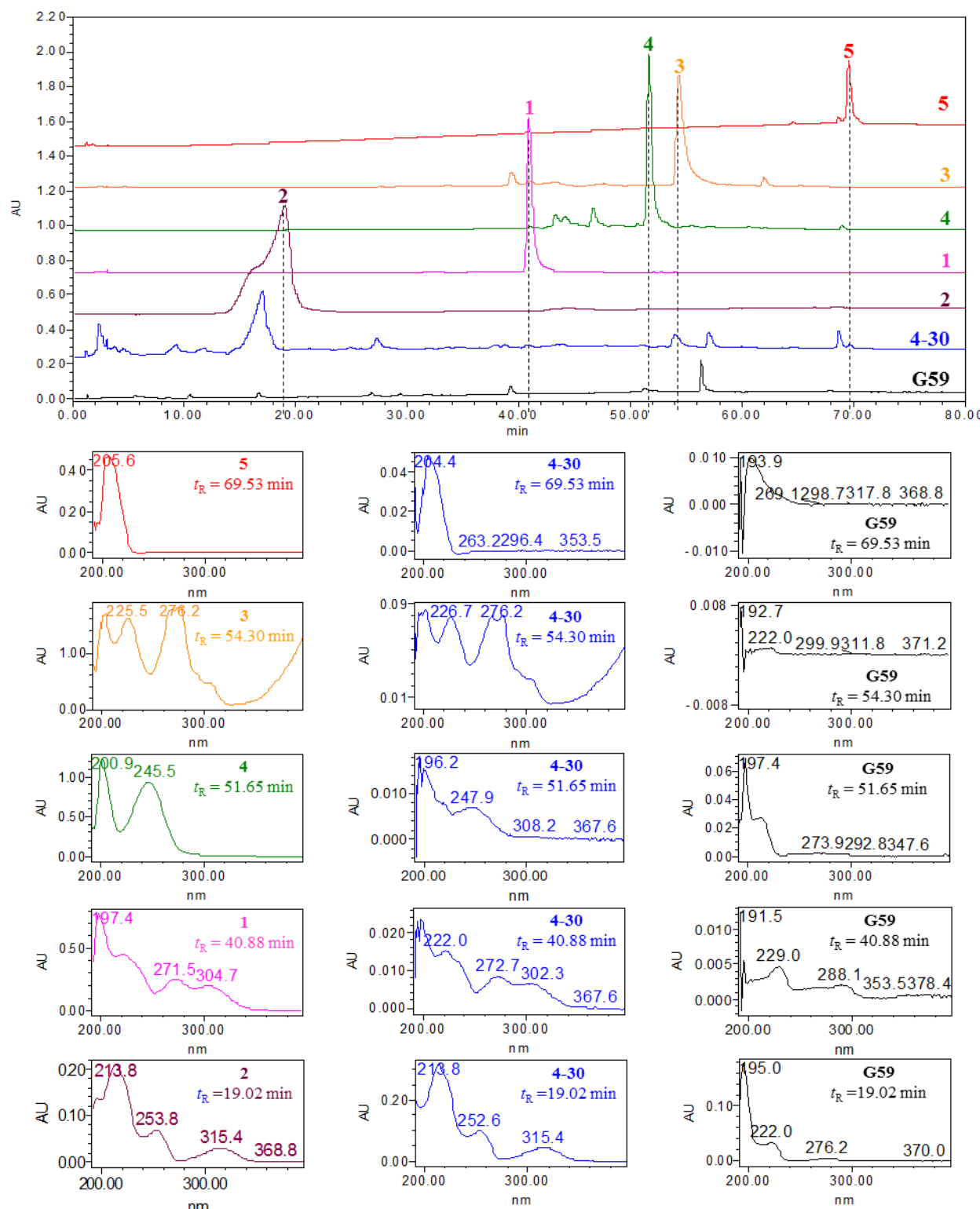
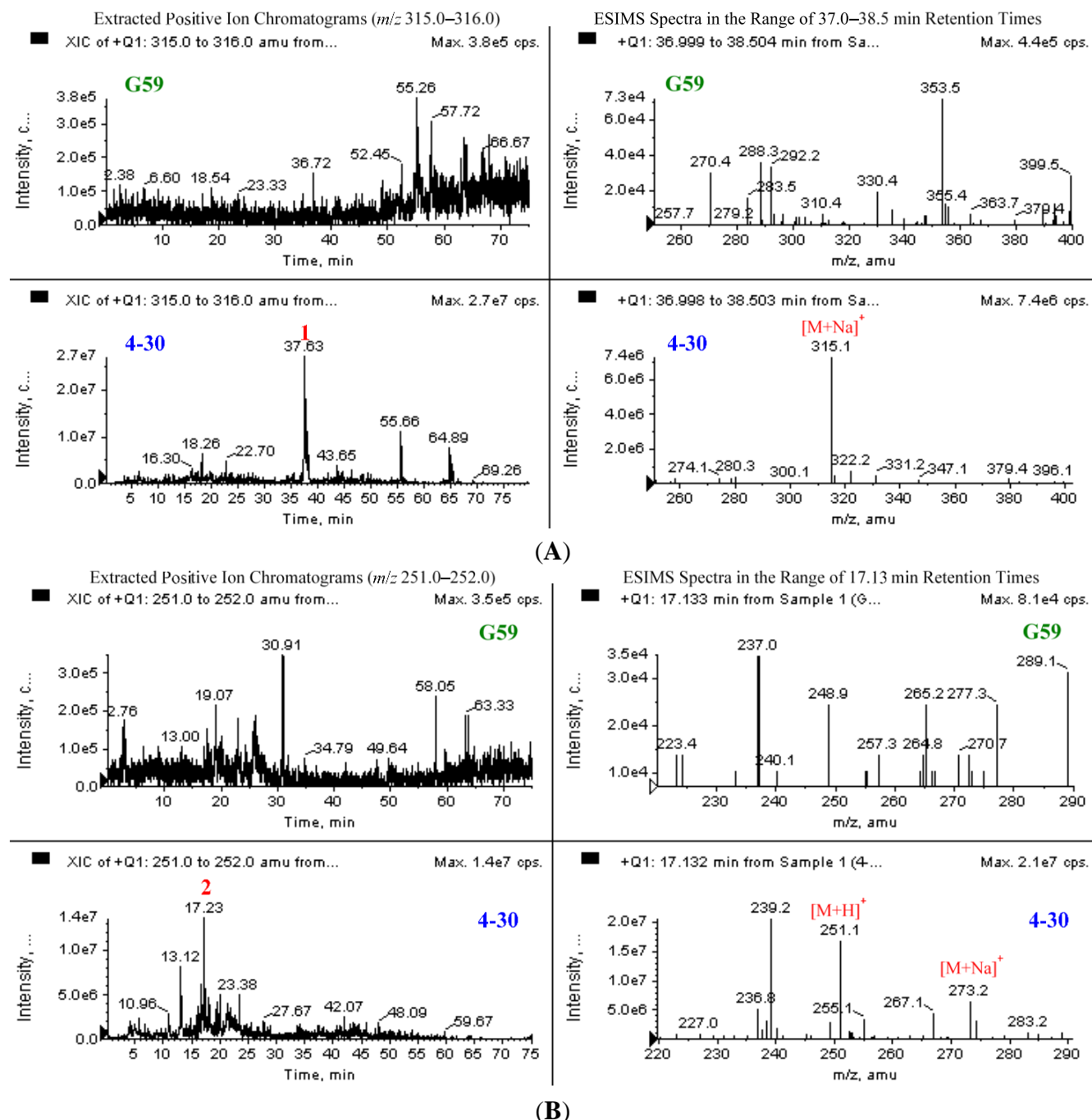


Figure S3. HPLC-PDAD-UV analysis of the EtOAc extracts of mutant 4-30 and the control G59 strain for detecting **1–5**. HPLC profiles of **1–5** and the EtOAc extracts of mutant 4-30 and the control G59 detected at 220 nm. UV spectra of **1–5** and the corresponding peaks in the mutant 4-30 and control G59 extracts.

**Figure S4. Cont.**

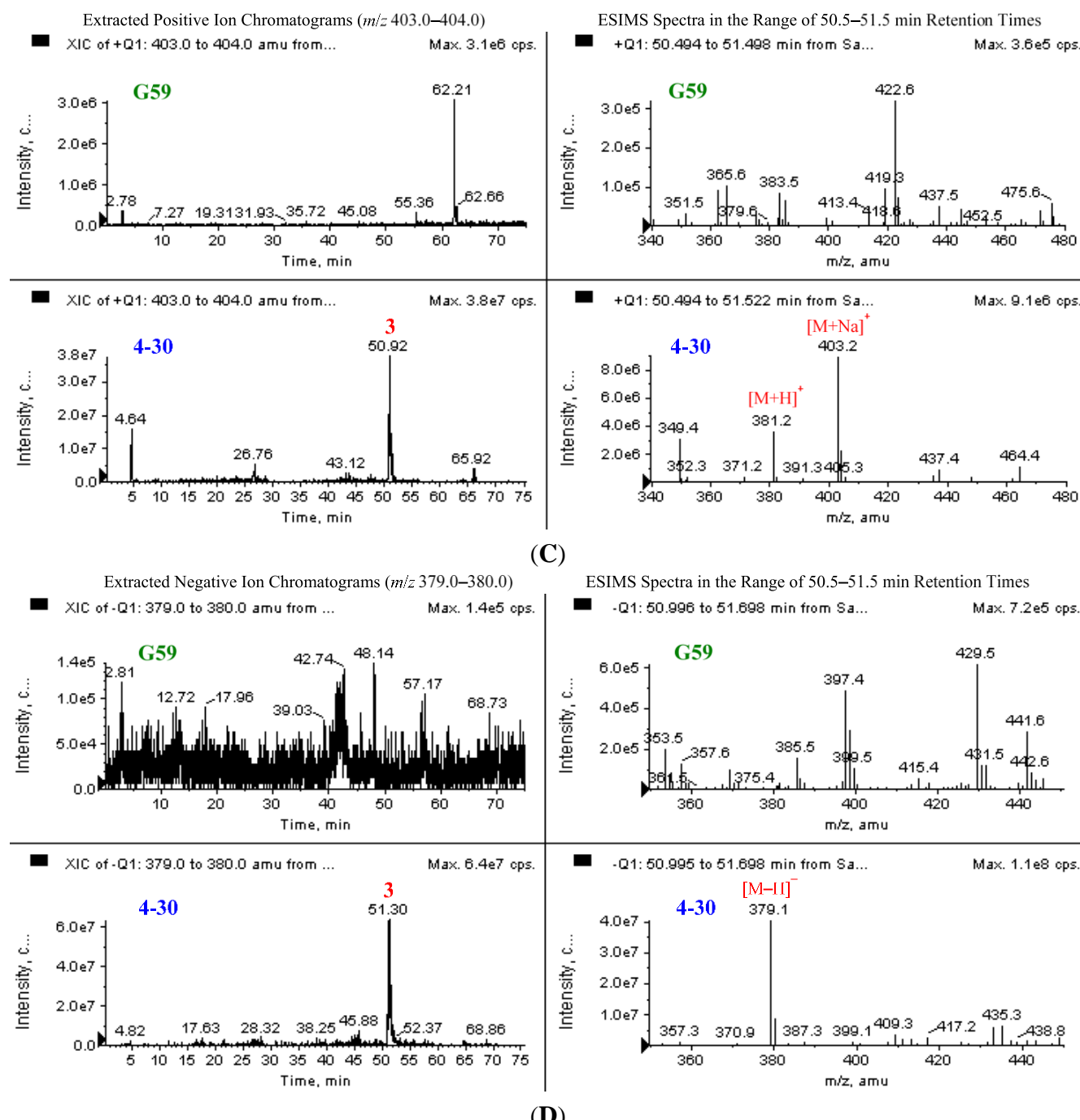


Figure S4. Cont.

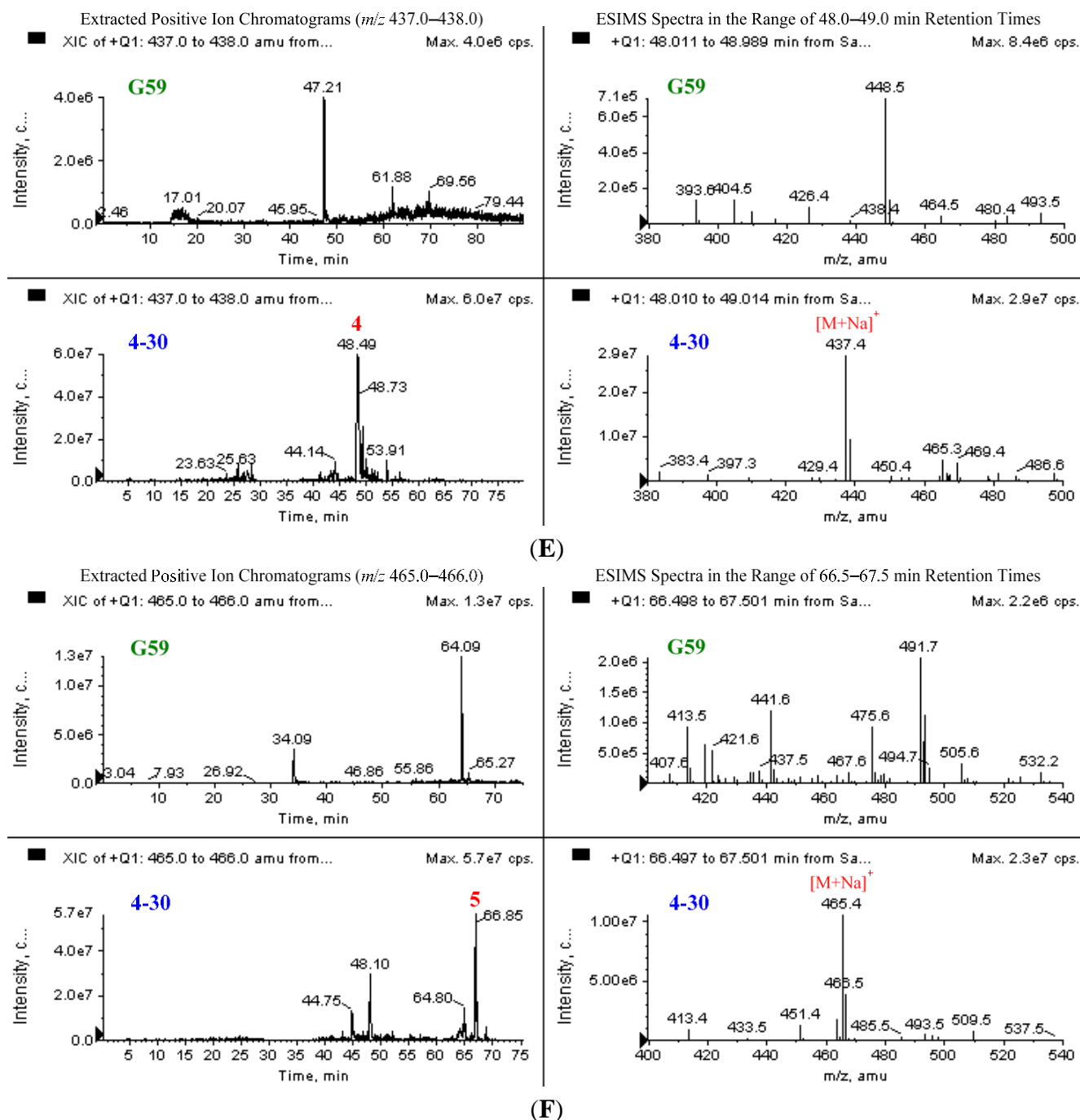


Figure S4. HPLC-ESI-MS analysis of the EtOAc extracts of mutant 4-30 and the control G59 strain for detecting **1–5**. (A) HPLC-Positive ion ESI-MS analysis (ESIMS m/z : 315 $[M + Na]^+$ for **1**); (B) HPLC-Positive ion ESI-MS analysis (ESIMS m/z : 251 $[M + H]^+$ for **2**); (C) HPLC-Positive ion ESI-MS analysis (ESIMS m/z : 403 $[M + Na]^+$ for **3**); (D) HPLC-Negative ion ESI-MS analysis (ESIMS m/z : 379 $[M - H]^-$ for **3**); (E) HPLC-Positive ion ESI-MS analysis (ESIMS m/z : 437 $[M + Na]^+$ for **4**); (F) HPLC-Positive ion ESI-MS analysis (ESIMS m/z : 465 $[M + Na]^+$ for **5**).